

1 **Research Article**

2

3

4 **PfGCN5, a global regulator of stress responsive genes, modulates artemisinin resistance**
5 **in *Plasmodium falciparum***

6 **Mukul Rawat¹, Abhishek Kanyal¹, Aishwarya Sahasrabudhe¹, Shruthi S. Vembar²,**

7 **Jose-Juan Lopez-Rubio³ and Krishanpal Karmodiya^{1§}**

8

9 **¹Biology Department, Indian Institute of Science Education and Research, Dr. Homi**

10 **Bhabha Road, Pashan, Pune 411 008, India.**

11 **²Institute for Bioinformatics and Applied Biotechnology, Bengaluru, Karnataka, India**

12 **³Dynamique des Interactions Membranaires Normales et Pathologiques, UMR5235**

13 **CNRS, INSERM, Université Montpellier, Montpellier, France.**

14

15 **§Corresponding author**

16 **Correspondence to: krish@iiserpune.ac.in**

17

18

19

20 **Running title: PfGCN5 modulates artemisinin resistance**

21

22 **Keywords:** Malaria; *Plasmodium falciparum*; Histone acetyltransferase; PfGCN5; Stress
23 response; Antigenic variation; and Drug Resistance.

24

25 **Abstract**

26 *Plasmodium falciparum* has evolved resistance to almost all front-line drugs including
27 artemisinins, which threatens malaria control and elimination strategies. Oxidative stress and
28 protein damage responses have emerged as key players in the generation of artemisinin
29 resistance. In this study, we show that PfGCN5, a histone acetyltransferase, binds to the stress
30 responsive and multi-variant family genes in poised state and regulates their expression under
31 stress conditions. We have also provided biochemical and cellular evidences that PfGCN5
32 regulates stress responsive genes by acetylation of PfAlba3. Furthermore, we show that upon
33 artemisinin exposure, genome-wide binding sites for PfGCN5 are increased and it is directly
34 associated with the genes implicated in artemisinin resistance generation like BiP and TRiC
35 chaperone. Moreover, inhibition of PfGCN5 in artemisinin resistant parasites, Kelch13
36 mutant, K13I543T and K13C580Y (RSA~ 25% and 6%, respectively) reverses the sensitivity
37 of the parasites to artemisinin treatment indicating its role in drug resistance generation.
38 Together, these findings elucidate the role of PfGCN5 as a global chromatin regulator of
39 stress-responses with potential role in modulating artemisinin drug resistance, and identify
40 PfGCN5 as an important target against artemisinin resistant parasites.

41

42 **Author Summary**

43 Malaria parasites are constantly adapting to the drugs we used to eliminate them. Thus, when
44 we use the drugs to kill parasites; with time, we select the parasites with the favourable
45 genetic changes. Parasites develop various strategies to overcome exposure to the drugs by
46 exhibiting the stress responses. The changes specific to the drug adapted parasites can be
47 used to understand the mechanism of drug resistance generation. In this study, we have
48 identified PfGCN5 as a global transcriptional regulator of stress responses in *Plasmodium*
49 *falciparum*. Inhibition of PfGCN5 reverses the sensitivity of the parasites to the artemisinin
50 drug and identify PfGCN5 as an important target against artemisinin resistant parasites.

51

52

53

54

55

56

57

58

59

60 **Introduction**

61 Malaria is a life threatening infectious disease caused by parasites from the genus
62 *Plasmodium*, with an estimated 200 million cases worldwide [1]. The *Anopheles* mosquito
63 serves as a vector for varied species of the human malaria parasite namely *P. falciparum*, *P.*
64 *vivax*, *P. ovale*, *P. malariae* and *P. knowlesi*. Of these five species, *P. falciparum* causes most
65 lethal form of malaria. The *Plasmodium* life cycle consists of two phases, sexual and asexual
66 in mosquitoes and humans, respectively. Since *Plasmodium* completes its life cycle in two
67 different hosts, it requires mechanisms for coordinated modulation of gene expression [2]. An
68 efficient transcriptional and post-transcriptional regulation of gene expression enables it to
69 establish chronic infection in humans [3, 4]. Moreover, recent studies have attested the
70 importance of epigenetic mechanisms in regulation of gene expression [3, 5, 6].
71 Morphological changes observed during the development of the malaria parasite in
72 erythrocytes are also governed by the fine-tuning of gene expression [2]. Furthermore, most
73 of the genes in *Plasmodium* are reported to be poised (genes exhibit high levels of histone
74 activation marks but no transcription), which favors the plasticity of its gene expression
75 programs [5, 7, 8].

76

77 During the asexual life cycle, when *Plasmodium* is developing within mature red blood cells
78 (RBCs), it is exposed to different kinds of environmental and physiological stresses. For
79 instance, during the trophozoite stage (18 h post-erythrocyte invasion (hpi)), the parasite
80 converts hemoglobin to hemozoin, leading to the accumulation of reactive oxygen species
81 (ROS) and consequently oxidative stress [9]. Various drugs like artemisinin, arteether etc.
82 used for antimalarial treatment also lead to similar ROS build up, ultimately killing the
83 parasite [9-11]. Another characteristic of malarial infection is the acute cyclical episodes of
84 fever, with an increase in temperature to 41 degrees Celsius for about 2-6 hours. This

85 periodic febrile response is triggered by the release of merozoites from RBCs [12, 13]. Since
86 *Plasmodium* faces these stress conditions during each of its infectious cycle, it has possibly
87 evolved mechanisms to resist the metabolic perturbations caused thereby. Interestingly, these
88 stress responses are also known to mediate resistance against various antimalarial drugs [14,
89 15]. Several classical antimalarial drugs like chloroquine [16], sulfadoxine-pyrimethamine
90 [17] and mefloquine [18] are no longer effective against *P. falciparum* [19, 20]. Currently,
91 artemisinin based combination therapy is considered as the last line of defense against *P.*
92 *falciparum* malaria [20]. However, since 2009, alarming reports of resistance against
93 artemisinin have emerged in Southeast Asia. This region has historically served as the
94 epicenter for emergence of anti-malarial drug resistance [21-23]. Recent reports from Eastern
95 India have also suggested the presence of artemisinin resistant parasites based on
96 pharmacokinetic and genetic parameters like increased parasite clearance half-life and novel
97 Kelch13 mutations [24, 25].

98

99 Currently, there is limited knowledge on the mechanism by which the parasites develop
100 resistance against artemisinin. Artemisinin resistant parasites are characterized by slow
101 growth and reduced drug susceptibility at the ring stage of asexual growth [15]. Artemisinin
102 resistant parasites are also shown to have extensive transcriptional deregulation, with
103 transcriptional regulators emerging as important players in the evolution of drug resistance
104 [26-29]. Multiple transcriptomics studies have revealed dormancy, oxidative stress response
105 and protein metabolism to be key players in mechanism of artemisinin drug resistance
106 generation [22, 26, 27, 29-31]. Unfortunately, the global transcriptional regulators of drug
107 resistance generation remain unexplored in *P. falciparum*. Previous studies in higher (e.g.,
108 humans) and lower (e.g., *Toxoplasma gondii*) eukaryotes demonstrated that GCN5, a histone
109 acetyltransferase plays an important role during stress conditions, where it has been

110 associated with high level of transcriptional reprogramming required for stress adaptation
111 [32-35]. GCN5 is conserved in *Plasmodium* species and till date, only two subunits of the
112 GCN5 complex, namely PfGCN5 and PfADA2 are identified [36, 37]. Previous studies using
113 DNA microarray have suggested that there is a weak but positive correlation between
114 PfGCN5 and H3K9ac mark [38]. In this study, we dissected role of PfGCN5 under various
115 physiological stress conditions in *P. falciparum* during intraerythrocytic development cycles.
116 With the help of chromatin immunoprecipitation coupled high-throughput sequencing (ChIP-
117 seq) and transcriptomic (RNA-sequencing) analyses, we show that PfGCN5 activates genes
118 that are important for the maintenance of parasite cellular homeostasis during various stress
119 conditions. Furthermore, we elucidate the role of PfAlba3 as the mediator of PfGCN5-
120 dependent regulation of stress responsive genes. Collectively, our data identify histone
121 acetyltransferase, PfGCN5 as a key chromatin regulator of stress responsive genes and
122 reveals its important role in emergence of artemisinin drug resistance.

123

124 **Results**

125 **PfGCN5 is associated with virulence and stress responsive genes**

126 While paralogs of GCN5 are well studied in multiple systems, little is known about the
127 function of GCN5 in *P. falciparum*. PfGCN5, encoded by *PF3D7_0823300*, contains histone
128 acetyltransferase (HAT) and bromo (for binding to acetylated histones) domains at its C-
129 terminal end (S1A Fig) [37]. To gain further insight into the function of PfGCN5 during
130 asexual growth, we generated polyclonal antibodies against recombinant C-terminal HAT
131 and bromo domains (amino acid 1183-1448) of PfGCN5 (also called α -HAT antibody, S1A-
132 S1B Fig). We also raised polyclonal antibodies against a peptide from the N-terminal region
133 of PfGCN5 (amino acids 9-25; called α -peptide antibody; S1A Fig). Specificity of the

134 generated antibodies was determined by Western blotting using parasite lysate (S1C Fig), and
135 by immunoprecipitation coupled with mass spectroscopy.

136

137 Next, to comprehend the transcriptional regulation mechanisms of PfGCN5, we performed
138 chromatin immunoprecipitation coupled high-throughput sequencing (ChIP-seq) using the α -
139 HAT and α -peptide PfGCN5 antibodies. ChIP-seq was performed at early trophozoite stage
140 (24 hpi) of parasite growth as PfGCN5 exhibits high mRNA expression at this stage (S2A
141 Fig) [39]. Peaks of local enrichment of PfGCN5 were determined after sequence alignment
142 and normalization to input sequences using the MACS2 peak calling software. In total, we
143 identified 754 high confidence common binding sites (fold enrichment ≥ 2 ; q value < 0.1)
144 with α -HAT and α -peptide PfGCN5 antibodies, which corresponds to 403 genes (S2B Fig).
145 The PfGCN5 bound sites using α -peptide PfGCN5 antibody are mentioned in S1 Table.
146 When we averaged PfGCN5 binding density for the α -HAT and α -peptide antibodies across
147 the average gene structure of *P. falciparum*, we observed identical profiles for the two (S2C
148 Fig). This confirmed that the antibodies are well-correlated and specifically recognize
149 PfGCN5.

150

151 Since different gene sets in *P. falciparum* have distinct histone modification distribution
152 profiles [5], we measured the signal density of H3K9ac, a histone modification that is known
153 to be mediated by PfGCN5, and compared it to PfGCN5 density distribution (as measured by
154 α -peptide antibody) across all 5712 *P. falciparum* genes. Interestingly, PfGCN5 was enriched
155 at the 3' end and centre of the gene body of the 403 target genes identified by MACS2
156 analysis. In contrast, these genes have the H3K9ac marks distributed along the entire gene
157 body (Fig1A, top panel). When compared with the heterochromatin protein (PfHP1)
158 occupancy, which uniformly coats chromosome ends that contain a majority of the multi-

159 copy variant genes (var, rifin and stevor), we found that PfGCN5 exhibits specific binding to
160 antigenic variation genes, as shown in the representative example for Chromosome 1 from
161 the trophozoite stage (Fig 1B). These results corroborate our earlier findings where we have
162 shown that stress and stimuli dependent genes show enrichment of histone modifications at
163 the centre and towards the 3'-end of the genes [5], while genes belonging to other
164 housekeeping functions demonstrate uniform distribution of histone modifications.

165

166 Further, to validate the peaks obtained in ChIP-seq, we performed ChIP-qPCR on randomly
167 selected genomic loci enriched for PfGCN5 and confirmed its binding (Fig 1C). Lastly, gene
168 ontology (GO) analysis of PfGCN5 bound genes indicated enrichment of terms such as
169 antigenic variation, stress response to heat, and response to unfolded proteins (Fig 1D),
170 suggesting that PfGCN5 may play a role in the regulation of stress responsive and stimuli-
171 dependent genes in *P. falciparum*. The presence of an expanded repertoire of GCN5-related
172 N-acetyltransferase (GNAT) family of histone acetyltransferases [40] clearly indicates the
173 possibility of uncharacterized HATs as writers of H3K9ac mark in *P. falciparum*.

174

175 **PfGCN5 is not a general transcription co-activator; it is specifically associated with**
176 **stress/stimuli associated genes**

177 Next, we investigated how PfGCN5 binding relates to transcriptional activity of a gene at the
178 trophozoite stage. We systematically calculated the enrichment levels of PfGCN5 and
179 H3K9ac, a general activation mark, at the gene body of all *P. falciparum* genes and compared
180 it to the relative expression levels of genes as evaluated by RNA-seq-based transcriptomic
181 analysis. As expected, we observed a positive correlation between H3K9ac enrichment and
182 the expression status of the downstream gene (Fig 2A; left panel). On the other hand, we did
183 not observe strong positive correlation between PfGCN5 gene-body occupancy and the

184 expression of nearby genes (Fig 2A; right panel). Genes with either high or low gene
185 expression levels (outlier points for log₂ read density) showed high PfGCN5 occupancy (Fig
186 2A), suggesting that PfGCN5 binds to both active and suppressed/poised genes. In order to
187 confirm this, we compared the expression levels of genes bound by PfGCN5 and contrasted
188 them with the expression of all the *P. falciparum* genes. The expression level of PfGCN5
189 bound genes spreads from high expression to low expression values (Fig 2B) indicating its
190 presence on expressed as well as suppressed genes. Interestingly, many of the PfGCN5 bound
191 genes have both activation (H3K9ac) and repression (H3K9me3) marks (Fig 2C), indicating
192 suppressed yet poised for future activation. Thus, absence of global correlation with
193 transcription and occupancy on suppressed/poised as well as active genes, suggest that
194 PfGCN5 is not a general transcriptional co-activator rather it may specifically regulate stress
195 responsive genes in *P. falciparum*.

196

197 **PfGCN5 is a specific regulator of stress responsive genes**

198 Next, we decided to look into the role of PfGCN5 during different stress conditions.
199 Synchronized ring stage parasites were exposed to two different physiological stress
200 conditions; temperature (40⁰C) and drug (30 nM artemisinin) exposure for 6 h. In order to
201 confirm the stress response we looked at the expression level of marker genes, which are
202 known to be upregulated during stress conditions in *Plasmodium*. For temperature stress we
203 looked at the expression level of the heat shock protein, HSP70 (S3A Fig) [13, 41]. Since the
204 artemisinin is known to induce oxidative stress through production of reactive oxygen
205 species, we confirmed the oxidative stress by validating the expression levels of glutathione
206 S-transferase and superoxide dismutase (S3A Fig) [42]. Interestingly, PfGCN5 was several
207 fold upregulated upon physiological stress conditions as shown by quantitative real-time PCR
208 (qPCR) using gene specific primers (Fig 3A). To identify the genes that are deregulated

209 under these stress conditions, we performed transcriptomic analysis using RNA-sequencing
210 and identified 727 and 942 genes (>2 fold change) deregulated upon artemisinin and high
211 temperature exposure, respectively (Fig 3B-3C). Genes showing deregulation during stress
212 conditions were also validated by qRT-PCR (S3B Fig). Most of the genes that are
213 upregulated during both artemisinin and temperature stress conditions are reported to
214 maintain cellular homeostasis (Fig 3B-3C; S2 Table). To further dissect the functional
215 correlation between transcriptome deregulation and recruitment of PfGCN5 under different
216 stress conditions, we performed ChIP-sequencing for PfGCN5 using α -peptide antibody
217 during both temperature and artemisinin stress conditions. Notably, most of these genes
218 which are bound by PfGCN5, are upregulated under artemisinin and temperature stress
219 conditions (Fig 3D), indicating that PfGCN5 is associated with the activation of stress
220 responsive genes.

221

222 Further to investigate the role of PfGCN5 during stress conditions, we overexpressed HAT
223 and bromo domains of PfGCN5 under normal and stress conditions as previous attempts
224 failed to knockout GCN5 in *P. berghei* and *P. falciparum* indicating it is essential for parasite
225 survival [43, 44]. Remarkably, we observed cell death upon overexpression of PfGCN5 HAT
226 and bromo domains during stress conditions (S3C Fig). This in turn suggests that
227 overexpression of PfGCN5 possibly leads to hyperactivation of stress responses, eventually
228 resulting in cell death.

229

230 **PfGCN5 helps in maintenance of homeostasis during artemisinin treatment**

231 Responses to oxidative stress and protein damage are shown to mediate emergence of
232 artemisinin resistance in malaria parasites [15, 28, 29, 45, 46]. Interestingly, 775 new
233 PfGCN5 bound sites were acquired under artemisinin stress conditions as indicated by ChIP-

234 sequencing of PfGCN5 (Fig 4A). Moreover, gene ontology of newly acquired PfGCN5
235 bound genes under artemisinin stress conditions includes pathways such as ubiquitin-
236 dependent protein catabolic process, cellular response to stimuli and response to drug, which
237 are known to be deregulated in artemisinin resistant parasites (Fig 4B). Of interest is the
238 binding of PfGCN5 at BiP and T-complex protein 1 (TCP1) ring (TRiC) chaperone genes. It
239 is plausible that the higher expression of PfGCN5 upregulates BiP and TRiC chaperones, thus
240 assisting the unfolded protein response in artemisinin resistant parasites [28]. This indicates
241 that PfGCN5 might be playing an important role in the emergence of artemisinin resistance
242 by regulating stress responsive pathways in *P. falciparum*.

243

244 Furthermore, to understand the role of PfGCN5 in artemisinin drug resistance, we decided to
245 use PfGCN5 inhibitor, garcinol. It is a specific inhibitor of PfGCN5 and showed an IC₅₀ of
246 ~15 μM [47] (S4A-S4B Fig). We performed the quantitative RT-PCR during stress
247 conditions both in presence and absence of garcinol (10μM). We found that both BiP and
248 TCP1 β (T complex protein 1 subunit beta) were upregulated during the stress conditions (Fig
249 4C-4D). Interestingly, under garcinol treatment there is a decrease expression levels of BiP
250 and TCP1 β under stress conditions (Fig 4C-4D).

251

252 Further to dissect the role of PfGCN5 in artemisinin drug resistance emergence and
253 maintenance, we looked at transcript level of PfGCN5 in artemisinin resistant lines.
254 Interestingly, PfGCN5 is upregulated in artemisinin resistant lines; K13-I543T (MRA-1241,
255 RSA~25%) and K13-C580Y (MRA-1236, RSA~6%) by 2.5 and 1.5 fold than their sensitive
256 counterparts, respectively (Fig 4E). We wondered if the inhibition of PfGCN5 activity
257 resulted in change in drug sensitivity of the artemisinin resistant lines: K13-I543T and K13-
258 C580Y. Ring survival assay (RSA) was performed in absence and presence of garcinol (used

259 a concentration which has no or minimal effect on normal parasite growth). We observed
260 36.4% decreases in the level of resistance for K13-I543T artemisinin resistant line in the
261 presence of PfGCN5 inhibitor, garcinol (Fig 4Fi). Interestingly, garcinol treatment of the
262 artemisinin resistant parasites, K13-C580Y completely reverses the artemisinin resistance
263 (Fig 4Fii) indicating that PfGCN5 plays an important role in artemisinin resistance.

264

265 In order to further understand the role of PfGCN5 in artemisinin resistance, we performed
266 PfGCN5 CHIP sequencing in artemisinin resistant K13-I543T (MRA-1241) and K13-C580Y
267 (MRA-1236) and their artemisinin sensitive counterpart K13-I543wt (MRA-1253) and K13-
268 C580wt (MRA1254). We investigated the strain specific genes enriched for PfGCN5 binding
269 and called their associated biological processes through the gene ontology analysis. Several
270 biological processes were found to be conserved between the sensitive and resistant strain.
271 These primarily include cellular adhesion, response to stimulus and antigenic variation,
272 highlighting their regulation by PfGCN5 across strains (Fig 4G). Interestingly, a set of genes
273 are uniquely enriched for PfGCN5 occupancy in the resistant strains. While, PfGCN5 is
274 enriched on cellular metabolism and protein translation associated genes in K13-I543T strain,
275 in K13-C580Y it is enriched on genes involved in vesicle fusion, and morphogenesis (Fig
276 4G). Deregulation of these biological pathways has been shown to be crucial for resistance
277 acquisition in the field isolates of *P. falciparum* [30, 48]. Thus, our findings also reiterate an
278 important aspect of resistance emergence posited earlier, that it is highly dynamic and can be
279 shaped by independent underlying genetic and external environmental factors [14]. Together,
280 these results suggest that PfGCN5 plays an important role in the regulation of stress
281 responses, which are associated with drug resistance emergence.

282

283

284 **PfGCN5 interacts with PfAlba3 and regulates its chromatin binding**

285 PfGCN5 has an unusually large N-terminal tail as compared to GCN5 in higher eukaryotes as
286 well as other members of the phylum Apicomplexa. This large N-terminal region of PfGCN5
287 might play an additional role in protein-protein interactions to regulate *Plasmodium*-specific
288 pathways. Further to understand the PfGCN5 mediated transcriptional regulation and to
289 identify its interacting partners, we performed immunoprecipitation-coupled mass
290 spectrometry using the two anti-PfGCN5 antibodies, α -HAT and α -peptide. We identified
291 approximately 125 proteins interacting specifically with PfGCN5 (S3 Table), representing
292 four major pathways namely chromatin assembly, response to stimuli, metabolic pathways
293 and translation regulation (S5A Fig). Interestingly, one of the family of proteins identified as
294 the interacting partners of PfGCN5 is PfAlba (Acetylation lowers binding affinity). PfAlbas
295 are known to play diverse role during transcriptional and translational regulation [49, 50].
296 Alba proteins are also known to play important role in stress response pathways in higher
297 eukaryotic system [51, 52]. As PfGCN5 was found to be majorly associated with stress
298 responsive genes, we decided to further study PfGCN5 and PfAlba3 interaction.

299

300 First, to validate the interaction of PfGCN5 with PfAlba3, we cloned, expressed and purified
301 recombinant His-tagged PfAlba3. As we were unable to express the full length PfGCN5 due
302 to its large size, we cloned and overexpressed GST-tagged HAT and bromo domains of
303 PfGCN5 (S1B Fig). Surprisingly, *in vitro* binding assay using recombinant His-tagged
304 PfAlba3 and GST-tagged PfGCN5-HAT did not show any interaction (Fig 5A). Thus, it is
305 possible that PfAlba3 either interacts with PfGCN5 outside of the HAT and bromodomain or
306 it interacts indirectly with the PfGCN5 complex *in vivo*. Next, we performed
307 immunoprecipitation using PfGCN5 peptide antibody and looked for PfAlba3 as its
308 interacting partner in the pulled down fractions by Western blotting. As shown in Fig 5B,

309 PfGCN5 co-elutes with PfAlba3 indicating an interaction with the PfGCN5 complex.
310 Furthermore, immunofluorescence analysis suggested a partial colocalisation of PfGCN5 and
311 PfAlba3 at trophozoite stages of *P. falciparum* (Fig 5C). Lastly, to understand the
312 physiological role of PfGCN5 and PfAlba3 interaction, we performed *in vitro*
313 acetyltransferase assays with the PfGCN5 complex and found that PfGCN5 indeed acetylates
314 PfAlba3 (Fig 5D). Together, these data suggest that PfGCN5 interacts with PfAlba3 and
315 mediates its acetylation.

316

317 Further to comprehend PfGCN5-mediated regulation of PfAlba3, we performed chromatin-
318 immunoprecipitation using anti-PfGCN5 or anti-PfAlba3 antibodies. Previous studies [13] as
319 well as our RNA sequencing data suggest that temperature stress results in deregulation of
320 stress responsive and multicopy variant (var) genes. Importantly, virulence genes are known
321 to be enriched for PfAlba occupancy and our data suggests enrichment of PfGCN5 (Fig 1D),
322 hinting at involvement of the two factors in var expression regulation [49]. Thus, to explore
323 the possible crosstalk between PfGCN5 and PfAlba3 in regulation of virulence and stress
324 responsive genes, cells were subjected to temperature stress at 16 hpi for a period of 6 hours (
325 5B Fig). This was followed by ChIP and qPCR with anti-PfGCN5 (peptide antibody) and
326 anti-PfAlba3 (protein antibody) antibodies. Interestingly, we observed an increased
327 occupancy of PfGCN5 and a corresponding decreased occupancy of PfAlba3 at stress
328 responsive and virulence genes under temperature stress condition (Fig 5E). Thus, the
329 interplay between PfGCN5 and PfAlba3 may play an important role in the regulation of
330 various stress responsive and virulence genes depending on external cues.

331

332

333

334 **Discussion**

335 **PfGCN5 is a stress/stimuli specific regulator and not a general transcriptional**
336 **coactivator**

337 *Plasmodium* must have evolved efficient machineries to overcome changes in environmental
338 conditions experienced in two different hosts. The ability of *Plasmodium* to develop
339 resistance against artemisinin is attributed to the competent stress responsive pathways and
340 the unfolded protein response machinery, which are activated upon artemisinin exposure [14,
341 15]. Here, we establish the role of the histone acetyltransferase PfGCN5 as a global regulator
342 of stress responsive pathways in *P. falciparum*. Genome-wide analysis of PfGCN5
343 occupancy shows that it is associated with stress responsive and multivariant gene family
344 (virulence genes). Interestingly, PfGCN5 occupancy at various genomic loci was found to
345 establish a transcriptionally poised state, which may allow these genes to be switched on or
346 off immediately in response to stimuli. Such regulation is crucial for the genes implicated in
347 stress response and host immune evasion. We and others have previously shown that
348 H3K14ac, another histone modification mediated by GCN5, is specifically present on poised
349 stress responsive genes in higher eukaryotic systems [53, 54] indicating a conserved role of
350 GCN5 in *P. falciparum*. Together, these results suggest that PfGCN5 is not a general
351 transcription coactivator and it specifically regulates the stress responsive and multicopy
352 variant (virulence) genes in *P. falciparum*.

353

354 **PfGCN5 is an important modulator of artemisinin resistance**

355 In order to get insights into the role of PfGCN5, we looked at the level of PfGCN5 transcript
356 as well as genome wide binding sites during stress conditions i.e. heat stress and artemisinin
357 exposure. We found that PfGCN5 is upregulated during stress conditions and its transcript
358 level is comparable to artemisinin resistant parasite. Surprisingly, upon artemisinin treatment

359 PfGCN5 is enriched on the genes important for the development of resistance against
360 artemisinin. Corroborating PfGCN5 genome-wide binding with transcriptome data during
361 stress conditions clearly indicates that PfGCN5 is associated with the genes which are
362 upregulated during stress conditions (e.g. artemisinin exposure). Furthermore, upon
363 interfering with the activity of PfGCN5 using its specific inhibitor, garcinol, we found a
364 significant decrease in the level of artemisinin resistance in the K13-I543T mutant (MR4-
365 1241, RSA-25%) and K13-C580Y (MRA-1236, RSA-6%). This in turn suggests that
366 PfGCN5 is a global regulator of stress responsive genes, and plays an important role in
367 artemisinin resistance maintenance.

368

369 Bhattacharjee *et al.* recently reported the amplified presence of PI3P vesicles which helps in
370 mitigating the protein damage due to artemisinin treatment [48]. These vesicles house
371 proteins like Kelch13, PfEMP1, BiP and others proteins required for maintaining homeostasis
372 in artemisinin resistant parasite. Proteome analysis of these vesicles has revealed a list of
373 proteins interacting with each other and possibly helping in emergence of artemisinin
374 resistance [55]. PfGCN5 is one of the proteins detected in the vesicular proteome. We found
375 a significant overlap in the proteins identified in the proteome analysis and PfGCN5
376 interacting partners (S6B Fig). In consonance, we also found various stress regulators such
377 as heat shock proteins and Albas as interacting partners of PfGCN5. These interactions may
378 play an important role in activation of stress response pathways upon artemisinin exposure.
379 Moreover, PfGCN5 also regulates transcription regulation of BiP and T complex protein 1
380 beta subunit beta under stress conditions. Reports from higher eukaryotic systems have
381 suggested that acetylation of BiP results in its dissociation from the protein kinase RNA-like
382 endoplasmic reticulum kinase (PERK), which further results in phosphorylation of eIF2alpha
383 leading to translation repression [56]. Moreover, we also found PfGCN5 to be enriched at

384 the promoter of the Kelch13 gene, which possibly hints at its transcriptional regulation.
385 Together, it suggests that PfGCN5 may play an important role in drug resistance generation
386 either by directly regulating the expression of the genes important for
387 emergence/maintenance of artemisinin resistance and/or by interacting with various key
388 stress-regulators involved in resistance generation in *P. falciparum* (Fig 6).

389

390 **PfGCN5 regulates virulence gene expression upon stress induction**

391 *Plasmodium falciparum* has evolved an extensive machinery to evade the host immune
392 system through changes in the expression of multicopy variant proteins (var, rifin and stevor),
393 which are expressed on the surface of infected RBCs [57, 58]. A switch in expression of these
394 proteins also helps the parasite in evading splenic and immune clearance by a process called
395 antigenic variation. Though the environmental cues responsible for virulence gene switching
396 are not known, several factors have been identified to play regulatory roles in antigenic
397 variation under physiological conditions [10, 57]. Various histone modifying enzymes like
398 PfSir2, PfHda2, PfSET2 and PfSET10 are shown to repress expression of virulence genes
399 [59-62]. *P. falciparum* heterochromatin protein 1 (HP1) is another key player known to
400 repress the expression of virulence genes by binding to H3K9me2/3 and
401 heterochromatinization [63, 64]. Here, we have identified PfGCN5 as a regulator of virulence
402 gene expression switch under temperature stress condition.

403

404 Furthermore, we also found PfAlba3, a DNA/RNA binding protein, as an interacting partner
405 of PfGCN5. PfAlba superfamily is known to play an important role in translation regulation
406 in *P. falciparum* [50, 65]. Moreover, acetylation of PfAlba3 is known to lower its binding to
407 DNA and results in gene activation [49]. Conversely, PfSir2a deacetylates PfAlba3 and
408 makes it competent to bind DNA and leads to gene suppression [49]. Here we show that

409 PfGCN5 binds to stress responsive and virulence genes and most probably regulates their
410 expression by the acetylation of PfAlba3. Thus, the interplay between PfGCN5, PfSir2A and
411 PfAlba3 possibly helps in regulation of stimuli dependent and virulence genes contributing to
412 stress responsive and virulence phenotype.

413

414 Several studies in prokaryotes have investigated the link between virulence and resistance
415 generation [66, 67]. There are clear evidences that virulence modulates resistance level in
416 microorganisms and *vice versa* suggesting that there is a mechanism which tightly regulates
417 both the processes. Geisinger *et al.* has showed the presence of a key stress response system
418 in *Acinetobacter baumannii*, which enhances the virulence and resistance level in response to
419 different physiological stresses [68]. Similarly, in *P. falciparum*, drug sensitivity of parasites
420 is shown to be virulence dependent, where virulent parasites are shown to have higher
421 likelihood to survive drug treatment [69]. Thus, it is plausible that regulation of both
422 virulence as well stress responsive genes, which are responsible for drug resistance
423 generation is mediated by same machinery involving GCN5 in *P. falciparum*.

424

425 Emergence of drug resistance against artemisinin is one of the biggest hurdles in malaria
426 control and eradication. Recent reports have implicated stress responsive pathways in drug
427 resistance generation (Fig 6). Understanding the regulation of stress responses and virulence
428 gene expression is crucial to fathom the pathogenesis of the parasites. Our study identifies
429 PfGCN5 as a global regulator of transcription of stress responses and virulence genes in *P.*
430 *falciparum*. The outcome of this study could potentially be used to develop and screen
431 inhibitors against drug resistant malaria parasites, which is one of the most prevalent parasitic
432 diseases in the world.

433

434 **Experimental Procedures**

435 **Parasite culture and transfection**

436 *P. falciparum* strain 3D7 was cultured as previously described [70]. Briefly, parasites were
437 cultured in RPMI1640 medium supplemented with 25 mM HEPES, 0.5 % AlbuMAX I, 1.77
438 mM sodium bicarbonate, 100 μ M hypoxanthine and 12.5 μ g ml⁻¹ gentamicin sulfate at 37 °C.
439 Parasites were sub-cultured after every two days. Subculturing was done by splitting the flask
440 into multiple flasks in order to maintain parasitemia around 5%. Hematocrit was maintained
441 to 1 -1.5% by adding freshly washed O +ve human RBC isolated from healthy human donor.
442 Synchronization was done with the help of 5% sorbitol in ring stage. Late stage
443 synchronization was performed using the Percoll density gradient method (63%). Parasitemia
444 was monitored using Giemsa staining of thin blood smear.

445

446 **Antibodies**

447 Anti-actin (Sigma A2066) and Anti-Rabbit IgG (OSB PM035) were used for Western
448 blotting and immunoprecipitation, respectively. Goat Anti-Rabbit Alexa Fluor 647 (A21245),
449 Goat anti-Rat Alexa Fluor 488 (A 11006), Goat Anti-Rabbit Alexa Fluor 488 (A11034) were
450 used for immunofluorescence. Rabbit polyclonal antibodies against PfAlba3 resulting from
451 immunizations of rabbits with the KLH-conjugate peptide IGKRMFTGNEEKNP were
452 obtained from GenScript Corporation [65]. Rat polyclonal antibodies against full-length
453 recombinant GST-tagged PfAlba3 were from GenScript Corporation. For generating PfGCN5
454 peptide antibody, online software LBtope was used for selecting the antigenic peptide.
455 PfGCN5 peptide (CEYCNVLYDGNELLRKRK) used for raising antibody was obtained
456 from Apeptide Co., Ltd., China. PfGCN5 peptide was conjugated to Keyhole limpet
457 hemocyanin (KLH) carrier protein for the immunization purpose. Both Anti-GCN5 peptide
458 and protein antibodies were raised at The National Facility for Gene Function in Health and

459 Disease, IISER Pune. The New Zealand White rabbits (3-4 months old) were used for
460 antibody generation. Antibodies were further purified using affinity chromatography on the
461 sulfolink resin.

462

463 **Western blotting**

464 Parasites were harvested using 0.15% saponin. Parasites pellets were washed using phosphate
465 buffer saline (PBS). Parasites were lysed using ice cold parasite lysis buffer (TRIS pH 8.0,
466 150 mM sodium chloride (NaCl), 0.5% nonyl phenoxyethoxyethanol (NP-40), 0.5%
467 sodium deoxycholate, 0.1 mM ethylenediaminetetraacetic acid, 1.5 mM magnesium chloride
468 ($MgCl_2$), 1X protease inhibitor cocktail (PIC) , 1 mM phenylmethylsulfonyl fluoride (PMSF).
469 Three freeze thaw cycles were performed using liquid nitrogen to achieve proper lysis of the
470 parasites. To get rid of debris, parasites were spun at 17949 x g for 30 minutes. Supernatant
471 was transferred to another tube. The lysate proteins were separated on 7.5% - 12%
472 polyacrylamide gels and transferred to PVDF membrane. The membrane was blocked using
473 5% skimmed milk and probed using primary antibody overnight at 4°C. After overnight
474 incubation membrane were washed using 1X Tris-buffered saline, 0.1% Tween 20 (TBST)
475 followed by 1hr incubation with secondary antibody in TBST (1:5000, Biorad). Three washes
476 were given for 10 minutes each after the secondary antibody incubation. Blots were
477 developed using Clarity Western ECL substrate (Biorad).

478

479 **Immunofluorescence Assay**

480 Parasites were fixed using 4% PFA and 0.00075% glutaraldehyde for 30 minutes at 37°C.
481 Permeabilisation was carried out using 0.1% Triton X-100 in PBS. Washing was performed
482 using 1X PBS after every step. Blocking was done using 3% BSA for 1hr at room
483 temperature followed by incubation with primary antibody in BSA for 3 hours. Three PBS

484 washes were given to remove the unbound primary antibody. Secondary antibody incubation
485 was done for 1 hour at room temperature. Parasites were washed before mounting on glass
486 slides using ProLong Gold Antifade with DAPI (Invitrogen).

487

488 **Quantitative RT-PCR**

489 RNA isolation was carried out using TRIzol reagent (Biorad). 2 µg of DNase free RNA was
490 used for cDNA synthesis using ImProm-II Reverse transcription system (Promega), as per the
491 manufacture's recommendation. Random primers were used for the cDNA synthesis. Real
492 time PCR was carried out using CFX96 Real Time PCR detection system (Biorad). 18S
493 rRNA and tRNA synthetase were used as an internal control to normalize for variability
494 across different samples. Quantification of the expression was done with the help of
495 fluorescence readout of SYBR green dye incorporation into the amplifying targets (Biorad).
496 Each experiment included technical triplicates and was performed over three independent
497 biological replicates. Primers details for the RT qPCR are given in S4 Table.

498

499 **Chromatin Immunoprecipitation**

500 Infected RBCs were crosslinked using 1% formaldehyde (Thermo Scientific, 28908) for 10
501 mins at RT. 150 mM glycine was added for quenching the cross-linking reaction. The
502 samples were washed using 1X PBS (chilled) before proceeding with lysis. Sample
503 homogenization was performed using swelling buffer (25 mM Tris pH 7.9, 1.5 mM MgCl₂,
504 10 mM KCL, 0.1% NP40, 1 mM DTT, 0.5 mM PMSF, 1x PIC) followed by cell lysis in
505 sonication buffer (10 mM Tris-HCl pH 7.5, 200 mM NaCl, 1 % SDS, 4 % NP-40, 1mM
506 PMSF, 1X PIC). Sonication was performed using Covaris S220 to obtain the chromatin size
507 of 200-400 bp. Pre-clearing was performed for 1 hour at 4⁰C using recombinant protein G
508 conjugated sepharose beads with continuous gentle inverting. 30 µg purified chromatin was

509 used per antibody (both α -HAT and α -peptide antibodies) and incubated for 12 h at 4⁰C.
510 Samples were then incubated with saturated Protein G Sepharose beads for 4 hours at 4⁰C.
511 Bound chromatin was finally washed and eluted using ChIP elution buffer (1 % SDS, 0.1 M
512 sodium bicarbonate). Both IP sample and input were reverse crosslinked using 0.3M NaCl
513 overnight at 65⁰C along with RNase. Proteinase K treatment was performed at 42⁰C for 1
514 hour. Finally DNA was purified using phenol chloroform precipitation. Target sites identified
515 from ChIP sequencing analysis were further validated by ChIP-qPCR using the Biorad SYBR
516 Green Master Mix (Biorad). Primers details for the ChIP-qPCR are provided in S5 Table.
517 Gene ontology was performed using PlasmoDB (www.plasmodb.org). Gene ontology terms
518 along with number of genes in each category are given in S6 Table and S7 Table.

519

520 **ChIP-sequencing Library preparation and sequencing**

521 ChIP-sequencing libraries for all the samples were prepared from 5-10 ng of DNA using the
522 NEB Next Ultra II DNA Library Prep kit. Chromatin immunoprecipitated, fragmented DNA
523 samples were end repaired and adapters ligated. Size selection was performed using
524 Agencourt XP beads (Beckman Coulter). Adapter ligated fragments were PCR amplified
525 using indexing primers followed by purification using the Agencourt XP beads (Beckman
526 Coulter). The library electropherograms were assessed using Agilent Bioanalyzer 2100 and
527 Agilent DNA 1000 kit. The libraries were pooled in equimolar concentration and 50 bp reads
528 were sequenced using Illumina HiSeq2500 (BENCOS Research Solutions Pvt. Ltd.,
529 Maharashtra).

530

531 **Data pre-processing and peak calling**

532 ChIP-seq data were mapped to *Plasmodium falciparum* 3D7 genome version 37
533 (<http://plasmodb.org/plasmo/>) using Bowtie2 with default parameters. The mapped reads

534 were used for peak calling against an input control data, using the MACS2 peak calling
535 software (default parameters) [71]. Peaks were annotated using Bedtools [72]. ChIP-seq
536 signals were background subtracted using MACS2 bdgcmp tool and the significantly
537 enriched peaks were visualized using Integrative Genomics Viewer (IGV).

538

539 **Average profile calculations**

540 We extracted the tag density in a 5 kb window surrounding the gene body using the
541 seqMINER tool which generates heatmap as well as the enrichment profiles of factors over
542 gene bodies [73]. For average gene profiles, genes (+/-5000 bp from binding site) were
543 divided in 100 bins relative to the gene length. Moreover 10 equally sized (50 bp) bins were
544 created on the 5' and 3' of the gene and ChIP-seq densities were collected for each dataset in
545 each bin.

546

547 **Data source and analysis**

548 ChIP seq data for Heterochromatin protein 1 (HP1) trophozoite stage was downloaded from
549 Gene Expression Omnibus (<http://www.ncbi.nlm.nih.gov/gds>) with accession number:
550 GSM2743113. Histone modification ChIP-seq data sets were downloaded from database
551 under the accession number GSE63369. seqMINER [73] was used for generating scatter plots
552 and average gene occupancy profiles. Correlation analysis and box plot were generated using
553 'R' software (<http://r-project.org/>).

554

555 **Stress induction**

556 Parasites were subjected to heat and therapeutic (artemisinin treatment) stresses for 6 hours
557 from late ring (~17 hrs) to early trophozoite (~23 hrs) stage. Double synchronization was

558 carried out to achieve tight synchronization of parasite stages. Parasites were exposed to a)
559 Heat stress (40°C for 6 hours) and b) Therapeutic stress (30 nM artemisinin for 6 hours).

560

561 **RNA sequencing and Data analysis**

562 Parasites were harvested for RNA isolation after 6 hours of stress induction. Total RNA was
563 isolated using TRIzol reagent according to the protocol. DNase treated RNA was used for
564 cDNA synthesis. Quality of the RNA was verified using Agilent Bioanalyzer 2100. Three
565 biological replicates were pooled together for performing RNA sequencing. The cDNA
566 libraries were prepared for samples using Illumina TruSeq RNA library preparation kit.
567 Transcriptome sequencing was performed using Illumina NextSeq 500 system (1x150 bp
568 read length) at BioServe Biotechnologies (India) Pvt Ltd. Hyderabad in replicate. Quality
569 control of the RNA-sequencing reads was performed using FASTQC and reads were trimmed
570 based on the quality estimates. The quality verified reads were then mapped onto the
571 reference genome (PlasmoDB_v37) using the HISAT2 software (New Tuxedo Suite). After
572 verification of the mapping percentage, the alignment data (SAM format) was converted into
573 its binary counterpart (BAM format) using samtools. The same step also sorts the aligned
574 reads positionally according to their genomic coordinates, making them easier to process
575 further. In order to quantify the reads mapped onto the genomic features (genes, exons, etc.),
576 the htseq-count feature was used. The count data was then used to perform differential gene
577 expression (DGE) analysis and statistical validation using the Deseq2 package in the R
578 computational environment. MA plot is generated using 'R' software (<http://r-project.org/>).

579

580 **Immunoprecipitation**

581 In order to harvest the parasites, infected RBCs were lysed using 0.15% saponin at 37°C.
582 Harvested parasites were then lysed using ice cold parasite lysis buffer (20 mM TRIS pH 8.0,

583 150 mM NaCl, 0.5% NP-40, 0.5% sodium deoxycholate, 0.1 mM EDTA, 1.5 mM MgCl₂, 1X
584 PIC, 1 mM PMSF). Lysed parasites were then centrifuged at 20817 x g for 30min at 4°C. Pre-
585 clearing was performed using recombinant protein G conjugated sepharose beads for 1 hour
586 at 4°C. Precleared lysate was then used for overnight incubation with antibody at 4°C. After
587 the overnight incubation of lysate with antibody, sepharose Protein G beads were added to
588 the lysate for 4 hours incubation. Washes were done using immunoprecipitation buffer (25
589 mM TRIS pH 7.9, 5 mM MgCl₂, 10% glycerol, 100 mM KCl, 0.1% NP-40, 0.3 mM DTT)
590 followed by elution of the proteins using glycine (pH – 2.5). Eluted proteins were neutralized
591 using 1 M Tris pH 8.8. For mass spectrometry analysis samples were digested with trypsin
592 for 16 hrs at 37°C. The digested samples were cleared using C18 silica cartridge. Peptides
593 were then analysed using EASY-nLC 1000 system (Thermo Fisher Scientific) coupled to
594 QExactive mass spectrometer (Thermo Fisher Scientific) equipped with nanoelectrospray ion
595 source (Valerian Chem Private Limited, New Delhi). Immunoprecipitation followed by mass
596 spectrometry was performed in three biological replicates. Samples were processed and RAW
597 files generated were analyzed with Proteome Discoverer against the Uniprot P.falci reference
598 proteome database. For Sequest search, the precursor and fragment mass tolerances were set
599 at 10 ppm and 0.5 Da, respectively. The protease used to generate peptides, i.e. enzyme
600 specificity was set for trypsin/P (cleavage at the C terminus of “K/R: unless followed by “P”)
601 along with maximum missed cleavages value of two. Carbamidomethyl on cysteine as fixed
602 modification and oxidation of methionine and N-terminal acetylation were considered as
603 variable modifications for database search. Both peptide spectrum match and protein false
604 discovery rate were set to 0.01 FDR.

605

606

607

608 **Protein expression and purification**

609 PfGCN5 (HAT and bromodomain) DNA sequence was amplified from parasite genomic
610 DNA using gene specific primers. The PCR-amplified fragment was cloned in frame with
611 glutathione S-transferase (GST) fusion protein in pGEX-4T1 plasmid vector using XhoI and
612 BamHI restriction enzymes. For expression in *E.coli*, pGEX-4T1 (GCN5) plasmid was
613 transformed in BL21 (DE3) star competent cells. Expression was induced at an optical
614 density of 0.6 at 600 nm, with 0.5 mM isopropyl-1-thio- β -d-galactopyranoside (IPTG) for 5
615 hrs at 25°C. Protein was purified using glutathione sepharose 4B beads (GE healthcare life
616 science). 20 mM concentration of reduced glutathione was used for protein elution. PfAlba3
617 was cloned in pET28a⁺ vector using NdeI and XhoI. Histidine-tagged PfAlba3 was expressed
618 in the *E. coli* BL21 (DE3) competent cells. Expression was induced at an optical density of
619 0.6 at 600nm, with 0.5 mM IPTG for 5 hours at 25°C. Protein purification was performed
620 using Ni-NTA beads. Protein was eluted using different concentration of Imidazole. Purified
621 proteins were dialyzed and stored at -20°C. Primers details for the cloning are provided in S8
622 Table.

623

624 ***In vitro* interaction assay**

625 *In vitro* interaction study was carried out using GST-tagged PfGCN5 and His tagged Alba3
626 proteins. Recombinant proteins (2ug) were incubated together overnight at 4°C. GST protein
627 was used as the negative control. Glutathione beads were added to the protein mix for 4 hours
628 at 4°C. The beads were washed and the bound proteins were eluted from the beads using 20
629 mM reduced glutathione. Western blotting was performed using Anti-His antibody to verify
630 presence of PfAlba3 in the elutions.

631

632 **Ring stage survival assay (RSA)**

633 *In vitro* RSA was performed according to the protocol described in Witkowski *et al.* (2013)
634 [74]. Parasites were synchronized at early ring stage. Tightly synchronised 0-3 hrs rings were
635 given 700 nM of artemisinin for 6 hrs. Drug was washed after 6 hrs with RPMI. Culture was
636 then cultivated for 66 hrs. Parasites were then lysed and the parasite growth was calculated
637 with the help of SYBR green I reagent which intercalates with the DNA and gives a
638 fluorescent readout upon excitation. Parasite survival rate was calculated comparing the
639 growth between drug treated and untreated control.

640

641 **Data access**

642 ChIP-sequencing data for PfGCN5 as well as gene expression data (RNA sequencing) for
643 different conditions are submitted to Sequence Read Archive (SRA) under ID SUB5640877.

644

645 **Ethics Statement**

646 This study does not involve human participants. Human RBCs used in this study were
647 obtained from the KEM Blood Bank (Pune, India) as blood from anonymized donors.
648 Approval to use this material for *P. falciparum in vitro* culture has been granted by the
649 Institutional Biosafety Committee of Indian Institute of Science Education and Research
650 Pune (BT/BS/17/582/2014-PID). The use of rabbits in this study for immunization
651 (IISER/IAEC/2017-01/008) was reviewed and approved by Indian Institute of Science
652 Education and Research (IISER)-Pune Animal House Facility (IISER: Reg No.
653 1496/GO/ReBi/S/11/CPCSEA). The approval is as per the guidelines issued by Committee
654 for the Purpose of Control and Supervision of Experiments on Animals (CPCSEA), Govt. of
655 India.

656

657 **Acknowledgements**

658 The following reagent was obtained through BEI Resources (www.mr4.org), NIAID, NIH:
659 *Plasmodium falciparum*, Strain IPC 3445 (MRA-1236), Strain IPC 4912 (MRA-1241),
660 contributed by Didier Menard and *Plasmodium falciparum*, Strain Cam2_rev (MRA-1254),
661 Strain IPC Cam2_rev (MRA-1253), contributed by David A. Fidock. We thank Dr. Artur
662 Scherf from Institut Pasteur, Paris, France, for his support. This work was supported by
663 grants under DST INSPIRE (IFA-13, LMBM-53) and DBT-IYBA (BT/08/IYBA/2014-17)
664 from Government of India to KK. MR is supported by DBT-SRF fellowship. MR is also
665 supported by EMBO short term fellowship to carry out part of this work. The funders had no
666 role in study design, data collection and analysis, decision to publish, or preparation of the
667 manuscript.

668

669 **Conflict of Interest**

670 The authors declare that they have no conflict of interest.

671

672

673

674

675

676

677

678

679 **Figure legends**

680 **Figure 1: *PfGCN5* is associated with virulence and stress responsive genes.** (A) Heat map
681 showing the ChIP-seq tag counts at 5712 *P. falciparum* genes for H3K9ac and *PfGCN5*.
682 *PfGCN5* was enriched only over a subset of genes having H3K9ac enrichment indicating that
683 it is not a general transcription co-activator. *PfGCN5* was found to be enriched mostly at the
684 3' end of the genes and towards the centre of the genes. (B) IGV browser snapshot of
685 representative genes having *PfGCN5* binding. Binding of H3K9ac, Heterochromatin protein
686 1 (HP1) and H3K9me3 are also represented for comparison on the same genes. (C) ChIP-
687 qPCR of selected genes confirms *PfGCN5* binding to ChIP-seq targets. The results are shown
688 as fold enrichment of ChIP performed with *PfGCN5* α -peptide antibody versus non-immune
689 IgG. (D) Gene ontology for the genes which were found to be bound by *PfGCN5* using ChIP
690 sequencing. Antigenic variation and other genes required during stress conditions are
691 overrepresented in gene ontology.

692

693 **Figure 2: *PfGCN5* is not a general transcription coactivator; it is specifically associated**
694 **with stimuli associated genes.** (A) Box and whisker plots representing the correlation of
695 genome-wide H3K9ac prevalence and *PfGCN5* occupancy with the global gene expression.
696 Absence of global correlation was found for the recruitment of *PfGCN5* and gene
697 expression. This indicates that *PfGCN5* is not a general transcription coactivator. (B) The
698 expression level of the genes bound *PfGCN5* in comparison to all genes in *P. falciparum* is
699 represented by the box plots. *PfGCN5* is associated with highly as well as least expressed
700 genes. (C) Scatter plot representing the correlation between the H3K9ac and H3K9me3
701 marks on *PfGCN5* bound genes. The plot indicates that many genes having *PfGCN5* binding
702 also have H3K9me3 marks suggesting that these genes are either suppressed or poised for
703 future activation.

704 **Figure 3: PfGCN5 is a specific stress regulator.** (A) Change in the expression level of
705 PfGCN5 during various stress conditions (N=3). PfGCN5 is found to be upregulated during
706 heat stress and artemisinin treatment conditions. Data shows the mean \pm SEM for three
707 independent experiments. (B) MA plot showing the deregulation in the expression of protein
708 coding genes during artemisinin treatment with 30nM concentration for 6 hours and (C)
709 during temperature stress at 40°C for 6 hours. (D) Expression profiles of the genes bound to
710 PfGCN5 during stress conditions. PfGCN5 bound genes are upregulated upon stress
711 induction as compared to control condition.

712

713 **Figure 4: PfGCN5 shows prolific genomic binding during artemisinin treatment and in**
714 **artemisinin resistant parasites.** (A) Venn diagram showing the number of genes occupied
715 by *PfGCN5* during normal conditions and during artemisinin treatment (30nM). (B) Gene
716 ontology of the genes which are exclusively bound to *PfGCN5* during artemisinin treatment.
717 *PfGCN5* is found to be enriched on the genes which are known to be deregulated in
718 artemisinin resistant parasites. This indicates the role of *PfGCN5* during resistance
719 generation. (C,D) RT-PCR results showing the upregulation of BiP and TCP1 β during stress
720 conditions and downregulation in the level of upregulation under garcinol treatment (10 μ M)
721 respectively. Data shows the mean \pm SEM for three independent experiments. (E) Transcript
722 level of expression of *PfGCN5* in artemisinin resistant strains, K13-I543T (MRA-1241) and
723 K13-C580Y (MRA-1236) in comparison to their sensitive counterparts, K13-I543wt (MRA-
724 1253) and K13-C580wt (MRA-1254), respectively. (F) Change in the percentage parasite
725 survival estimated through Ring Survival Assay (RSA) in presence of *PfGCN5* inhibitor
726 garcinol. i) K13-I543T (MRA-1241) parasites were treated with 5 μ M garcinol and ii) K13-
727 C580Y (MRA-1236) parasites were treated with 250 μ M garcinol. Presence of garcinol
728 decreases the artemisinin resistance in K13-I543T (MRA-1241) at a concentration which has

729 otherwise no effect on parasite growth. Higher concentration of garcinol was used with a
730 significant decrease in resistance level in K13-C580Y (MRA-1236) parasites. (G) Gene
731 ontology enrichment of the genes which are bound by PfGCN5 in K13-I543T (MRA-1241),
732 K13-C580Y (MRA-1236), K13-I543wt (MRA-1253), K13-C580wt (MRA-1254).

733

734 **Figure 5: PfGCN5 regulates the binding of PfAlba3 to DNA through acetylation.** (A) *In*
735 *vitro* binding assay of recombinant PfGCN5 (HAT and bromodomain) and PfAlba3.
736 Absence of binding was confirmed with Western blotting using Anti-His antibody. (B)
737 Immunoprecipitation was performed to confirm the interaction of PfGCN5 and PfAlba3.
738 PfGCN5 interacting proteins were pull down using PfGCN5 peptide antibody and binding
739 was confirmed with Western blotting using PfAlba3 antibody. (C) Immunofluorescence assay
740 was performed to check the localization of PfGCN5 and PfAlba3. Both the proteins were
741 found to colocalize at certain regions indicating the positive interaction between them.
742 PfGCN5 was visualized using Anti Rabbit Alexa 647 and PfAlba3 was labelled using Anti-
743 Rat Alexa 488. Nucleus was stained using DAPI. Images were further processed for
744 deconvolution using the Huygens Essential software. (D) Histone acetyltransferase (HAT)
745 assay to verify PfGCN5 mediated acetylation of PfAlba3. The assay was performed using
746 recombinant PfAlba3 and the PfGCN5 complex (pulled down with the help of PfGCN5
747 antibody). PfGCN5 was found to acetylate PfAlba3. (E) ChIP-qPCR showing the switching
748 in the PfGCN5 and PfAlba3 enrichment on multivariant/stress responsive genes under
749 temperature stress. ChIP was performed using PfGCN5 (peptide) and PfAlba3 antibodies.

750

751 **Figure 6: Mechanisms proposed for artemisinin resistance in *P. falciparum*.** Model
752 showing the role and interplay of Kelch13, PI3K and PfGCN5 in artemisinin resistance
753 generation. Artemisinin treatment leads to random alkylation of proteins, which in turn are

754 ubiquitinated by the protein ubiquitination complex (of which Kelch13 is an important ligase
755 adapter component) and subjected to degradation by proteosomal degradation. One such
756 protein is the PI3K (phosphatidylinositol 3 kinase), which is implicated in lipid metabolism
757 and cell survival signaling. Massive alkylation by artemisinin exposure and/or oxidative
758 stress activates PfGCN5 in the nucleus, which in turn upregulates the stress-responsive and
759 unfolded protein response pathways. Thus, mutations in Kelch13 as well as upregulation of
760 stress-responsive pathways by PfGCN5 help in artemisinin resistance generation.

761

762

763 References

- 764 1. WHO (2018) World Malaria Report.
- 765 2. Mamoun, C. B., Gluzman, I.Y., Hott, C., MacMillan, S.K., Amarakone, A.S., Anderson,
766 D.L., Carlton, J.M., Dame, J.B., Chakrabarti, D., Martin, R.K., Brownstein, B.H., Goldberg,
767 D.E. (2001) Co-ordinated programme of gene expression during asexual intraerythrocytic
768 development of the human malaria parasite *Plasmodium falciparum* revealed by microarray
769 analysis, *Molecular microbiology*. **39**, 26-36.
- 770 3. Coleman, B. I. & Duraisingh, M. T. (2008) Transcriptional control and gene silencing in
771 *Plasmodium falciparum*, *Cell Microbiol.* **10**, 1935-46.
- 772 4. Cui, L., Lindner, S. & Miao, J. (2015) Translational regulation during stage transitions in
773 malaria parasites, *Annals of the New York Academy of Sciences*. **1342**, 1-9.
- 774 5. Karmodiya, K., Pradhan, S. J., Joshi, B., Jangid, R., Reddy, P. C. & Galande, S. (2015) A
775 comprehensive epigenome map of *Plasmodium falciparum* reveals unique mechanisms of
776 transcriptional regulation and identifies H3K36me2 as a global mark of gene suppression,
777 *Epigenetics & chromatin*. **8**, 32.
- 778 6. Duffy, M. F., Selvarajah, S. A., Josling, G. A. & Petter, M. (2013) Epigenetic regulation
779 of the *Plasmodium falciparum* genome, *Briefings in functional genomics*. **13**, 203-216.
- 780 7. Volz, J. C., Bartfai, R., Petter, M., Langer, C., Josling, G. A., Tsuboi, T., Schwach, F.,
781 Baum, J., Rayner, J. C., Stunnenberg, H. G., Duffy, M. F. & Cowman, A. F. (2012) PfSET10,
782 a *Plasmodium falciparum* methyltransferase, maintains the active var gene in a poised state
783 during parasite division, *Cell Host Microbe*. **11**, 7-18.
- 784 8. Guizetti, J. & Scherf, A. (2013) Silence, activate, poise and switch! Mechanisms of
785 antigenic variation in *Plasmodium falciparum*, *Cell Microbiol.* **15**, 718-26.
- 786 9. Percário, S., Moreira, D. R., Gomes, B. A. Q., Ferreira, M. E. S., Gonçalves, A. C. M.,
787 Paula S. O. C. Laurindo, P. S. O. C., Vilhena, T. C., Dolabela, M. F. & Green, M. D. (2012)
788 Oxidative Stress in Malaria, *International Journal of Molecular Sciences*. **13**, 16346-16372.
- 789 10. Rosenberg, E., Ben-Shmuel, A., Shalev, O., Sinay, R., Cowman, A. & Pollack, Y. (2009)
790 Differential, positional-dependent transcriptional response of antigenic variation (var) genes
791 to biological stress in *Plasmodium falciparum*, *PLoS One*. **4**, e6991.
- 792 11. Beckera, K., Tilley, L., Vennerstrom, J. L., Roberts, D., Rogerson, S. & Ginsburg, H.
793 (2004) Oxidative stress in malaria parasite-infected erythrocytes: host-parasite interactions,
794 *International Journal for Parasitology* **34**, 163-189.
- 795 12. Engelbrecht, D. & Coetzer, T. L. (2013) Turning up the heat: heat stress induces markers
796 of programmed cell death in *Plasmodium falciparum* in vitro, *Cell Death Dis.* **4**, e971.
- 797 13. Oakley, M. S., Kumar, S., Anantharaman, V., Zheng, H., Mahajan, B., Haynes, J. D.,
798 Moch, J. K., Fairhurst, R., McCutchan, T. F. & Aravind, L. (2007) Molecular factors and
799 biochemical pathways induced by febrile temperature in intraerythrocytic *Plasmodium*
800 *falciparum* parasites, *Infect Immun.* **75**, 2012-25.
- 801 14. Rocamora, F., Zhu, L., Liong, K. Y., Dondorp, A., Miotto, O., Mok, S., Bozdech, Z.
802 Oxidative stress and protein damage responses mediate artemisinin resistance in malaria
803 parasites, *PLoS Pathog*, e1006930.
- 804 15. Dogovski, C., Xie, S. C., Burgio, G., Bridgford, J., Mok, S., McCaw, J. M., Chotivanich,
805 K., Kenny, S., Gnadig, N., Straimer, J., Bozdech, Z., Fidock, D. A., Simpson, J. A., Dondorp,
806 A. M., Foote, S., Klonis, N. & Tilley, L. (2015) Targeting the cell stress response of
807 *Plasmodium falciparum* to overcome artemisinin resistance, *PLoS Biol.* **13**, e1002132.
- 808 16. Wellems, T. E., Panton, L. J., Gluzman, I. Y., do Rosario, V. E., Gwadz, R. W., Walker-
809 Jonah, A. & Krogstad, D. J. (1990) Chloroquine resistance not linked to mdr-like genes in a
810 *Plasmodium falciparum* cross, *Nature*. **345**, 253-255.

- 811 17. Basco, L. K., Tahar, K. & Ringwald, P. (1998) Molecular Basis of In Vivo Resistance to
812 Sulfadoxine-Pyrimethamine in African Adult Patients Infected with Plasmodium
813 falciparum Malaria Parasites, *ANTIMICROBIAL AGENTS AND CHEMOTHERAPY*. **42**,
814 1811–1814.
- 815 18. Nosten, F., van Vugt, M., Price, R., Luxemburger, C., Thway, K. L., Brockman, A.,
816 McGready, R., ter Kuile, F., Looareesuwan, S. & White, N. J. (2000) Effects of artesunate-
817 mefloquine combination on incidence of Plasmodium falciparum malaria and mefloquine
818 resistance in western Thailand: a prospective study, *The Lancet*. **356**, 297-302.
- 819 19. Ridley, R. G. (2002) Medical need, scientific opportunity and the drive for antimalarial
820 drugs, *Nature*. **415**, 686-693.
- 821 20. Blasco, B., Leroy, D. & Fidock, D. A. (2017) Antimalarial drug resistance: linking
822 Plasmodium falciparum parasite biology to the clinic, *Nat Med*. **23**, 917-928.
- 823 21. Dondorp, A. M., Nosten, F., Yi, P., Das, D., Phyo, A. P., Tarning, J., Lwin, K. M., Arieu,
824 F., Hanpithakpong, W., Lee, S. J., Ringwald, P., Silamut, K., Imwong, M., Chotivanich, K.,
825 Lim, P., Herdman, T., An, S. S., Yeung, S., Singhasivanon, P., Day, N. P., Lindegardh, N.,
826 Socheat, D. & White, N. J. (2009) Artemisinin resistance in Plasmodium falciparum malaria,
827 *N Engl J Med*. **361**, 455-67.
- 828 22. Fairhurst, R. M. & Dondorp, A. M. (2016) Artemisinin-Resistant Plasmodium
829 falciparum Malaria, *Microbiol Spectr*. **4**.
- 830 23. Hanboonkunupakarn, B. & White, N. J. (2016) The threat of artemisinin resistant malaria
831 in Southeast Asia, *Travel Med Infect Dis*. **14**, 548-550.
- 832 24. Mishra, N., Prajapati, S. K., Kaitholia, K., Bharti, R. S., Srivastava, B., Phookan, S.,
833 Anvikar, A. R., Dev, V., Sonal, G. S., Dhariwal, A. C., White, N. J. & Valecha, N. (2015)
834 Surveillance of artemisinin resistance in Plasmodium falciparum in India using the kelch13
835 molecular marker, *Antimicrobial agents and chemotherapy*. **59**, 2548-53.
- 836 25. Das, S., Manna, S., Saha, B., Hati, A. K. & Roy, S. (2018) Novel pfkelch13 gene
837 polymorphism associates with artemisinin resistance in eastern India, *Clinical infectious
838 diseases : an official publication of the Infectious Diseases Society of America*.
- 839 26. Mok, S., Imwong, M., Mackinnon, M. J., Sim, J., Ramadoss, R., Yi, P., Mayxay, M.,
840 Chotivanich, K., Liong, K.-Y. & Russell, B. (2011) Artemisinin resistance in Plasmodium
841 falciparum is associated with an altered temporal pattern of transcription, *BMC genomics*. **12**,
842 391.
- 843 27. Phompradit, P., Chaijaroenkul, W. & Na-Bangchang, K. (2017) Cellular mechanisms of
844 action and resistance of Plasmodium falciparum to artemisinin, *Parasitol Res*. **116**, 3331-
845 3339.
- 846 28. Suresh, N., Haldar, K. (2018) Mechanisms of artemisinin resistance in Plasmodium
847 falciparum malaria, *Current Opinion in Pharmacology*, 46–54.
- 848 29. Mbengue, A., Bhattacharjee, S., Pandharkar, T., Liu, H., Estiu, G., Stahelin, R. V., Rizk,
849 S. S., Njimoh, D. L., Ryan, Y., Chotivanich, K., Nguon, C., Ghorbal, M., Lopez-Rubio, J. J.,
850 Pfrender, M., Emrich, S., Mohandas, N., Dondorp, A. M., Wiest, O. & Haldar, K. (2015) A
851 molecular mechanism of artemisinin resistance in Plasmodium falciparum malaria, *Nature*.
852 **520**, 683-7.
- 853 30. Mok, S., Ashley, E. A., Ferreira, P. E., Zhu, L., Lin, Z., Yeo, T., Chotivanich, K.,
854 Imwong, M., Pukrittayakamee, S. & Dhorda, M. (2015) Population transcriptomics of human
855 malaria parasites reveals the mechanism of artemisinin resistance, *Science*. **347**, 431-435.
- 856 31. Xue-Franzén, Y., Henriksson, J., Bürglin, T. R. & Wright, A. P. (2013) Distinct roles of
857 the Gcn5 histone acetyltransferase revealed during transient stress-induced reprogramming of
858 the genome, *BMC genomics*. **14**, 1471-2164.

- 859 32. Gaupel, A. C., Begley, T. J. & Tenniswood, M. (2015) Gcn5 Modulates the Cellular
860 Response to Oxidative Stress and Histone Deacetylase Inhibition, *J Cell Biochem.* **116**, 1982-
861 92.
- 862 33. Hu, Z., Song, N., Zheng, M., Liu, X., Liu, Z., Xing, J., Ma, J., Guo, W., Yao, Y., Peng,
863 H., Xin, M., Zhou, D. X., Ni, Z. & Sun, Q. (2015) Histone acetyltransferase GCN5 is
864 essential for heat stress-responsive gene activation and thermotolerance in Arabidopsis, *Plant*
865 *J.* **84**, 1178-91.
- 866 34. Johnsson, A., Xue-Franzen, Y., Lundin, M. & Wright, A. P. (2006) Stress-specific role
867 of fission yeast Gcn5 histone acetyltransferase in programming a subset of stress response
868 genes, *Eukaryot Cell.* **5**, 1337-46.
- 869 35. Naguleswaran, A., Elias, E. V., McClintick, J., Edenberg, H. J. & Sullivan, W. J., Jr.
870 (2010) Toxoplasma gondii lysine acetyltransferase GCN5-A functions in the cellular
871 response to alkaline stress and expression of cyst genes, *PLoS Pathog.* **6**, e1001232.
- 872 36. Fan, Q., An, L. & Cui, L. (2004) Plasmodium falciparum histone acetyltransferase, a
873 yeast GCN5 homologue involved in chromatin remodeling, *Eukaryot Cell.* **3**, 264-76.
- 874 37. Fan, Q., An, L. & Cui, L. (2004) PfADA2, a Plasmodium falciparum homologue of the
875 transcriptional coactivator ADA2 and its in vivo association with the histone
876 acetyltransferase PfGCN5, *Gene.* **336**, 251-61.
- 877 38. Cui, L., Miao, J., Furuya, T., Li, X., Su, X. Z. & Cui, L. (2007) PfGCN5-mediated
878 histone H3 acetylation plays a key role in gene expression in Plasmodium falciparum,
879 *Eukaryot Cell.* **6**, 1219-27.
- 880 39. Bartfai, R., Hoeijmakers, W. A., Salcedo-Amaya, A. M., Smits, A. H., Janssen-Megens,
881 E., Kaan, A., Treeck, M., Gilberger, T. W., Francoijs, K. J. & Stunnenberg, H. G. (2010)
882 H2A.Z demarcates intergenic regions of the plasmodium falciparum epigenome that are
883 dynamically marked by H3K9ac and H3K4me3, *PLoS Pathog.* **6**, e1001223.
- 884 40. Kanyal, A., Rawat, M., Gurung, P., Choubey, D., Anamika, K. & Karmodiya, K. (2018)
885 Genome-wide survey and phylogenetic analysis of histone acetyltransferases and histone
886 deacetylases of Plasmodium falciparum, *FEBS J.* **285**, 1767-1782.
- 887 41. Zininga, T., Achilonu, I., Hoppe, H., Prinsloo, E., Dirr, H. W. & Shonhai, A. (2015)
888 Overexpression, Purification and Characterisation of the Plasmodium falciparum Hsp70-z
889 (PfHsp70-z) Protein, *PLoS One.* **10**, e0129445.
- 890 42. Percario, S., Moreira, D. R., Gomes, B. A., Ferreira, M. E., Goncalves, A. C., Laurindo,
891 P. S., Vilhena, T. C., Dolabela, M. F. & Green, M. D. (2012) Oxidative stress in malaria,
892 *International journal of molecular sciences.* **13**, 16346-72.
- 893 43. Bushell, E., Gomes, A. R., Sanderson, T., Anar, B., Girling, G., Herd, C., Metcalf, T.,
894 Modrzynska, K., Schwach, F., Martin, R. E., Mather, M. W., McFadden, G. I., Parts, L.,
895 Rutledge, G. G., Vaidya, A. B., Wengelnik, K., Rayner, J. C. & Billker, O. (2017) Functional
896 Profiling of a Plasmodium Genome Reveals an Abundance of Essential Genes, *Cell.* **170**,
897 260-272 e8.
- 898 44. Zhang, M., Wang, C., Otto, T. D., Oberstaller, J., Liao, X., Adapa, S. R., Udenze, K.,
899 Bronner, I. F., Casandra, D., Mayho, M., Brown, J., Li, S., Swanson, J., Rayner, J. C., Jiang,
900 R. H. Y. & Adams, J. H. (2018) Uncovering the essential genes of the human malaria parasite
901 Plasmodium falciparum by saturation mutagenesis, *Science.* **360**.
- 902 45. Bridgford, J. L., Xie, S. C., Cobbold, S. A., Pasaje, C. F. A., Herrmann, S., Yang, T.,
903 Gillett, D. L., Dick, L. R., Ralph, S. A., Dogovski, C., Spillman, N. J. & Tilley, L. (2018)
904 Artemisinin kills malaria parasites by damaging proteins and inhibiting the proteasome, *Nat*
905 *Commun.* **9**, 3801.
- 906 46. Zhang, M., Gallego-Delgado, J., Fernandez-Arias, C., Waters, N. C., Rodriguez, A.,
907 Tsuji, M., Wek, R. C., Nussenzweig, V. & Sullivan, W. J., Jr. (2017) Inhibiting the

- 908 Plasmodium eIF2alpha Kinase PK4 Prevents Artemisinin-Induced Latency, *Cell Host*
909 *Microbe*. **22**, 766-776 e4.
- 910 47. Jeffers, V., Gao, H., Checkley, L. A., Liu, Y., Ferdig, M. T. & Sullivan, W. J. (2016)
911 Garcinol inhibits GCN5-mediated lysine acetyltransferase activity and prevents replication of
912 the parasite *Toxoplasma gondii*, *Antimicrobial agents and chemotherapy*. **60**, 2164-2170.
- 913 48. Bhattacharjee, S., Coppens, I., Mbengue, A., Suresh, N., Ghorbal, M., Slouka, Z.,
914 Safeukui, I., Tang, H. Y., Speicher, D. W., Stahelin, R. V., Mohandas, N. & Haldar, K.
915 (2018) Remodeling of the malaria parasite and host human red cell by vesicle amplification
916 that induces artemisinin resistance, *Blood*. **131**, 1234-1247.
- 917 49. Goyal, M., Alam, A., Iqbal, M. S., Dey, S., Bindu, S., Pal, C., Banerjee, A., Chakrabarti,
918 S. & Bandyopadhyay, U. (2012) Identification and molecular characterization of an Alba-
919 family protein from human malaria parasite *Plasmodium falciparum*, *Nucleic acids research*.
920 **40**, 1174-90.
- 921 50. Vembar, S. S., Macpherson, C. R., Sismeiro, O., Coppee, J. Y. & Scherf, A. (2015) The
922 PfAlba1 RNA-binding protein is an important regulator of translational timing in
923 *Plasmodium falciparum* blood stages, *Genome Biol*. **16**, 212.
- 924 51. Verma, J. K., Wardhan, V., Singh, D., Chakraborty, S. & Chakraborty, N. (2018)
925 Genome-Wide Identification of the Alba Gene Family in Plants and Stress-Responsive
926 Expression of the Rice Alba Genes, *Genes*. **9**.
- 927 52. Alves, L. R. & Goldenberg, S. (2016) RNA-binding proteins related to stress response
928 and differentiation in protozoa, *World journal of biological chemistry*. **7**, 78-87.
- 929 53. Karmodiya, K., Krebs, A.R., Oulad-Abdelghani, M., Kimura, H., Tora, L. (2012) H3K9
930 and H3K14 acetylation co-occur at many gene regulatory elements, while H3K14ac marks a
931 subset of inactive inducible promoters in mouse embryonic stem cells, *BMC genomics*. **13**,
932 1471- 2164.
- 933 54. Kuo, M. H., vom Baur, E., Struhl, K., Allis, C.D. (2000) Gcn4 Activator Targets Gcn5
934 Histone Acetyltransferase to Specific Promoters Independently of Transcription, *Molecular*
935 *Cell*. **6**, 1309-1320.
- 936 55. Zhang, M., Mishra, S., Sakthivel, R., Rojas, M., Ranjan, R., Sullivan, W. J., Jr.,
937 Fontoura, B. M., Menard, R., Dever, T. E. & Nussenzweig, V. (2012) PK4, a eukaryotic
938 initiation factor 2alpha(eIF2alpha) kinase, is essential for the development of the erythrocytic
939 cycle of *Plasmodium*, *Proc Natl Acad Sci U S A*. **109**, 3956-61.
- 940 56. Rao, R., Nalluri, S., Kolhe, R., Yang, Y., Fiskus, W., Chen, J., Ha, K., Buckley, K. M.,
941 Balusu, R. & Coothankandaswamy, V. (2010) Treatment with panobinostat induces glucose-
942 regulated protein 78 acetylation and endoplasmic reticulum stress in breast cancer cells,
943 *Molecular cancer therapeutics*, 1535-7163. MCT-09-0988.
- 944 57. Scherf, A., Hernandez-Rivas, R., Buffet, P., Bottius, E., Benatar, C., Pouvelle, B., Gysin,
945 J. & Lanzer, M. (1998) Antigenic variation in malaria: in situ switching, relaxed and mutually
946 exclusive transcription of var genes during intra-erythrocytic development in *Plasmodium*
947 *falciparum*, *The EMBO journal*. **17**, 5418-5426.
- 948 58. Deitsch, K. W. & Dzikowski, R. (2017) Variant gene expression and antigenic variation
949 by malaria parasites, *Annual review of microbiology*. **71**, 625-641.
- 950 59. Tonkin, C. J., Carret, C. K., Duraisingh, M. T., Voss, T. S., Ralph, S. A., Hommel, M.,
951 Duffy, M. F., da Silva, L. M., Scherf, A. & Ivens, A. (2009) Sir2 paralogs cooperate to
952 regulate virulence genes and antigenic variation in *Plasmodium falciparum*, *PLoS biology*. **7**,
953 e1000084.
- 954 60. Coleman, B. I., Skillman, K. M., Jiang, R. H., Childs, L. M., Altenhofen, L. M., Ganter,
955 M., Leung, Y., Goldowitz, I., Kafsack, B. F. & Marti, M. (2014) A *Plasmodium falciparum*
956 histone deacetylase regulates antigenic variation and gametocyte conversion, *Cell host &*
957 *microbe*. **16**, 177-186.

- 958 61. Volz, J. C., Bártfai, R., Petter, M., Langer, C., Josling, G. A., Tsuboi, T., Schwach, F.,
959 Baum, J., Rayner, J. C. & Stunnenberg, H. G. (2012) PfSET10, a Plasmodium falciparum
960 methyltransferase, maintains the active var gene in a poised state during parasite division,
961 *Cell host & microbe*. **11**, 7-18.
- 962 62. Jiang, L., Mu, J., Zhang, Q., Ni, T., Srinivasan, P., Rayavara, K., Yang, W., Turner, L.,
963 Lavstsen, T. & Theander, T. G. (2013) PfSETvs methylation of histone H3K36 represses
964 virulence genes in Plasmodium falciparum, *Nature*. **499**, 223.
- 965 63. Perez-Toledo, K., Rojas-Meza, A. P., Mancio-Silva, L., Hernandez-Cuevas, N. A.,
966 Delgadillo, D. M., Vargas, M., Martinez-Calvillo, S., Scherf, A. & Hernandez-Rivas, R.
967 (2009) Plasmodium falciparum heterochromatin protein 1 binds to tri-methylated histone 3
968 lysine 9 and is linked to mutually exclusive expression of var genes, *Nucleic acids research*.
969 **37**, 2596-606.
- 970 64. Flueck, C., Bartfai, R., Volz, J., Niederwieser, I., Salcedo-Amaya, A. M., Alako, B. T.,
971 Ehlgren, F., Ralph, S. A., Cowman, A. F., Bozdech, Z., Stunnenberg, H. G. & Voss, T. S.
972 (2009) Plasmodium falciparum heterochromatin protein 1 marks genomic loci linked to
973 phenotypic variation of exported virulence factors, *PLoS Pathog.* **5**, e1000569.
- 974 65. Chene, A., Vembar, S. S., Riviere, L., Lopez-Rubio, J. J., Claes, A., Siegel, T. N.,
975 Sakamoto, H., Scheidig-Benatar, C., Hernandez-Rivas, R. & Scherf, A. (2012) PfAlbas
976 constitute a new eukaryotic DNA/RNA-binding protein family in malaria parasites, *Nucleic
977 Acids Res.* **40**, 3066-77.
- 978 66. Schroeder, M., Brooks, B. D. & Brooks, A. E. (2017) The Complex Relationship
979 between Virulence and Antibiotic Resistance, *Genes (Basel)*. **8**.
- 980 67. Geisinger, E. & Isberg, R. R. (2017) Interplay Between Antibiotic Resistance and
981 Virulence During Disease Promoted by Multidrug-Resistant Bacteria, *J Infect Dis.* **215**, S9-
982 S17.
- 983 68. Geisinger, E., Mortman, N. J., Vargas-Cuevas, G., Tai, A. K. & Isberg, R. R. (2018) A
984 global regulatory system links virulence and antibiotic resistance to envelope homeostasis in
985 *Acinetobacter baumannii*, *PLoS Pathog.* **14**, e1007030.
- 986 69. Schneider, P., Chan, B. H., Reece, S. E. & Read, A. F. (2008) Does the drug sensitivity
987 of malaria parasites depend on their virulence?, *Malar J.* **7**, 257.
- 988 70. Radfar, A., Mendez, D., Moneriz, C., Linares, M., Marin-Garcia, P., Puyet, A., Diez, A.
989 & Bautista, J. M. (2009) Synchronous culture of Plasmodium falciparum at high parasitemia
990 levels, *Nat Protoc.* **4**, 1899-915.
- 991 71. Zhang, Y., Liu, T., Meyer, C. A., Eeckhoutte, J., Johnson, D. S., Bernstein, B. E.,
992 Nusbaum, C., Myers, R. M., Brown, M., Li, W. & Liu, X. S. (2008) Model-based analysis of
993 ChIP-Seq (MACS), *Genome Biol.* **9**, R137.
- 994 72. Quinlan, A. R. & Hall, I. M. (2010) BEDTools: a flexible suite of utilities for comparing
995 genomic features, *Bioinformatics.* **26**, 841-2.
- 996 73. Ye T, K. A., Choukrallah MA, Keime C, Plewniak F, Davidson I and Tora, L. (2011)
997 seqMINER: an integrated ChIP-seq data interpretation platform, *Nucleic Acids Res.* **39**, e35.
- 998 74. Witkowski, B., Amaratunga, C., Khim, N., Sreng, S., Chim, P., Kim, S., Lim, P., Mao,
999 S., Sopha, C., Sam, B., Anderson, J. M., Duong, S., Chuor, C. M., Taylor, W. R. J., Suon, S.,
1000 Mercereau-Puijalon, O., Fairhurst, R. M. & Menard, D. (2013) Novel phenotypic assays for
1001 the detection of artemisinin-resistant Plasmodium falciparum malaria in Cambodia: in-vitro
1002 and ex-vivo drug-response studies, *The Lancet Infectious Diseases.* **13**, 1043-1049.

1004

1005

1006 **Supporting Information Figure Legends**

1007 **Supplementary Table S1. PfGCN5 bound sites identified using ChIP sequencing.** ChIP
1008 sequencing of PfGCN5 using the α -peptide antibody was performed during early
1009 trophozoites. The sites identified to be bound by PfGCN5 are listed in the table according to
1010 their decreasing fold enrichment.

1011

1012 **Supplementary Table S2. Genes deregulated during stress conditions.** RNA sequencing
1013 was performed during stress conditions to identify the genes deregulated. List of genes along
1014 with their tag count is listed in table 2.

1015

1016 **Supplementary Table S3. PfGCN5 interacting proteins.** PfGCN5 interacting proteins were
1017 identified using the both PfGCN5 α -HAT and α -peptide antibody. List of proteins which
1018 were found using both these antibodies are mentioned in the table 3.

1019

1020 **Supplementary Table S4. Primers used in the study.** Sequences of the RT-PCR primers
1021 used in the study.

1022

1023 **Supplementary Table S5. Primers used in the study.** Sequences of the quantitative PCR
1024 primers used in this study.

1025

1026 **Supplementary Table S6. Genes identified in each gene ontology term.** Gene ontology of
1027 the genes bound with PfGCN5 was performed using Plasmodb. Number of genes which were
1028 found in each category of the gene ontology term is mentioned in the table.

1029

1030 **Supplementary Table S7. Genes identified in each gene ontology term.** Gene ontology of
1031 the genes bound with PfGCN5 exclusively during artemisinin treatment was performed using
1032 Plasmodb. Number of genes which were found in each category of the gene ontology term is
1033 mentioned in the table.

1034

1035 **Supplementary Table S8. Primers used for the cloning of PfGCN5.** Sequences of the
1036 primers used for cloning of PfGCN5 for protein expression and overexpression.

1037

1038

1039 **Supplementary Figures**

1040 **Supplementary Figure S1: *PfGCN5* specific antibody generation.** (S1A) Schematic
1041 diagram showing the domain organization of *PfGCN5*. Histone acetyltransferase
1042 (HAT) domain and bromodomain (represented in blue and orange colour, respectively) are
1043 present at C terminal end. *PfGCN5* peptide from N-terminal region of the protein was
1044 commercially synthesized for raising antibody. The HAT and bromodomain was cloned in
1045 pGEX 4T1 vector for expression of *PfGCN5* protein tagged with GST. Protein expression
1046 was induced using 0.5mM IPTG in BL21 (DE3) star competent cells. (S1B) Protein was
1047 purified using glutathione beads and eluted using reduced glutathione (20mM). Protein
1048 expression was confirmed using anti-GST Western blotting. Protein was further purified
1049 using electro elution before injected in rabbit for Anti-*PfGCN5* antibody generation. Single
1050 band protein (*PfGCN5*-GST) was observed after electro elution in SDS-PAGE. Antiserum
1051 raised against *PfGCN5* protein (HAT and bromodomain) was checked for specificity using
1052 bacterial lysate expressing *PfGCN5*. (S1C) Specificity of the antibody was further checked
1053 using parasite protein lysate from asynchronous culture. Western blotting result indicates the
1054 presence of more than one forms of *PfGCN5* in *Plasmodium*. Western blotting was
1055 performed on proteins which are pulled down by α -HAT antibody and probed with α -peptide
1056 antibody. The presence of full length band indicates that both antibodies detect full length
1057 *PfGCN5*. (S1D) Schematic to possibly explain the bands which are observed during Western
1058 blotting for both the antibodies generated again *PfGCN5*. (S1E) In order to check whether the
1059 extra bands observed in Western blotting are the result of possible proteosomal degradation,
1060 parasites were treated with MG132 inhibitor for different duration of time. MG132 treatment
1061 resulted in significant decrease in number of bands observed. Only two bands were observed
1062 after 24hr treatment of MG132 which might indicate two isoforms of *PfGCN5*.

1063 **Supplementary Figure S2: *PfGCN5* is associated with virulence and stimuli induced**
1064 **genes.** (S2A) Dynamics of *PfGCN5* transcript expression during different stages of

1065 intraerythrocytic life cycle of *P.falciparum*. Expression profile suggests the low expression of
1066 PfGCN5 during the ring stages and a sudden burst of PfGCN5 mRNA expression during
1067 early trophozoite stage. (S2B) Scatter plot depicting a linear correlation of the target tag
1068 densities in ChIP pulldown performed using the scores of overlapping peaks from the
1069 PfGCN5 HAT domain and peptide antibodies. This is indicative of the fact that both
1070 antibodies have similar pulldown profile in ChIP sequencing reads. (S2C) Heat map showing
1071 PfGCN5 occupancy over 403 genes identified as the targets using PfGCN5 (HAT) antibody
1072 and peptide antibody.

1073

1074 **Supplementary Figure S3: Differential gene expression during stress conditions.** (S3A)

1075 Different markers genes were found to be deregulated during stress conditions. Temperature
1076 stress results in up regulation of HSP70. Similarly artemisinin (ART) treatment results in the
1077 increase in expression of Glutathione S-transferase and Superoxide dismutase which indicates
1078 the presence of ROS in parasites due to artemisinin treatment. Up regulation of these markers
1079 genes is indicative of the fact that stress is induced in the parasite upon artemisinin treatment
1080 and increase in temperature. (S3B) RT-qPCR validation of the genes which are deregulated
1081 during stress conditions, identified through RNA sequencing. (S3C) Parasites with episomal
1082 overexpression of truncated PfGCN5 (HAT and bromodomain) exhibited cell death during
1083 stress conditions. Artemisinin (Art, 30nM) and Tert-Butyl hydroperoxide (TBO, 10mM) were
1084 given to parasites for 6 hrs. TBO was used to induce ROS stress in parasites.

1085

1086 **Supplementary Figure S4: Recombinant HAT domain of PfGCN5 is catalytically active**

1087 **and can be inhibited by garcinol treatment.** (S4A) Inhibition of histone acetylation activity
1088 of purified recombinant HAT domain of PfGCN5. 10 μ M of Garcinol inhibits PfGCN5 HAT

1089 activity completely. (S4B) IC50 calculation of garcinol using dose response assay carried out
1090 over a period of 48 hours. The growth inhibition was measured using the SYBR green dye.

1091

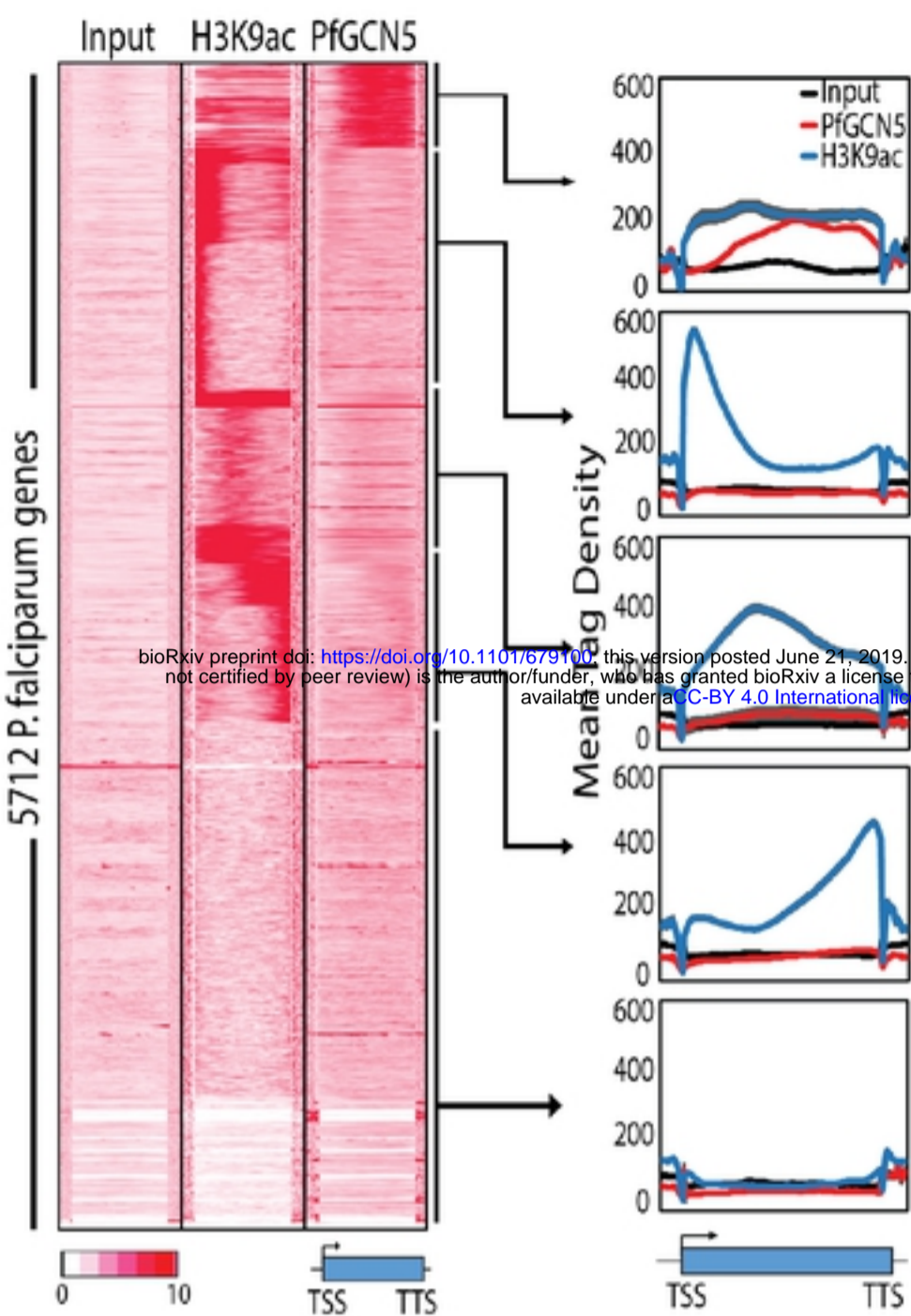
1092 **Supplementary Figure S5: Gene Ontology of the protein interactors of PfGCN5;**
1093 **validation of interaction of PfGCN5-PfAlba3 and investigating the expression of**
1094 **PfAlba3 targets in stress conditions.** (S5A) Gene ontology analysis of PfGCN5 interacting
1095 proteins indicate the overrepresentation of four major biological pathways namely chromatin
1096 assembly, response to stimuli, metabolic pathways and translation regulation. Gene ontology
1097 was performed using PlasmoDB and the plot was generated using Revigo
1098 (<http://revigo.irb.hr/>) (S5B) Immunofluorescence images to investigate the colocalisation of
1099 PfGCN5 and PfAlba3 show high rate for colocalisation, suggesting significant overlap
1100 between the two. (S5C) Change in the expression level of the various virulence genes during
1101 temperature stress. Temperature stress results in upregulation of more than one virulence
1102 genes in *Plasmodium*.

1103

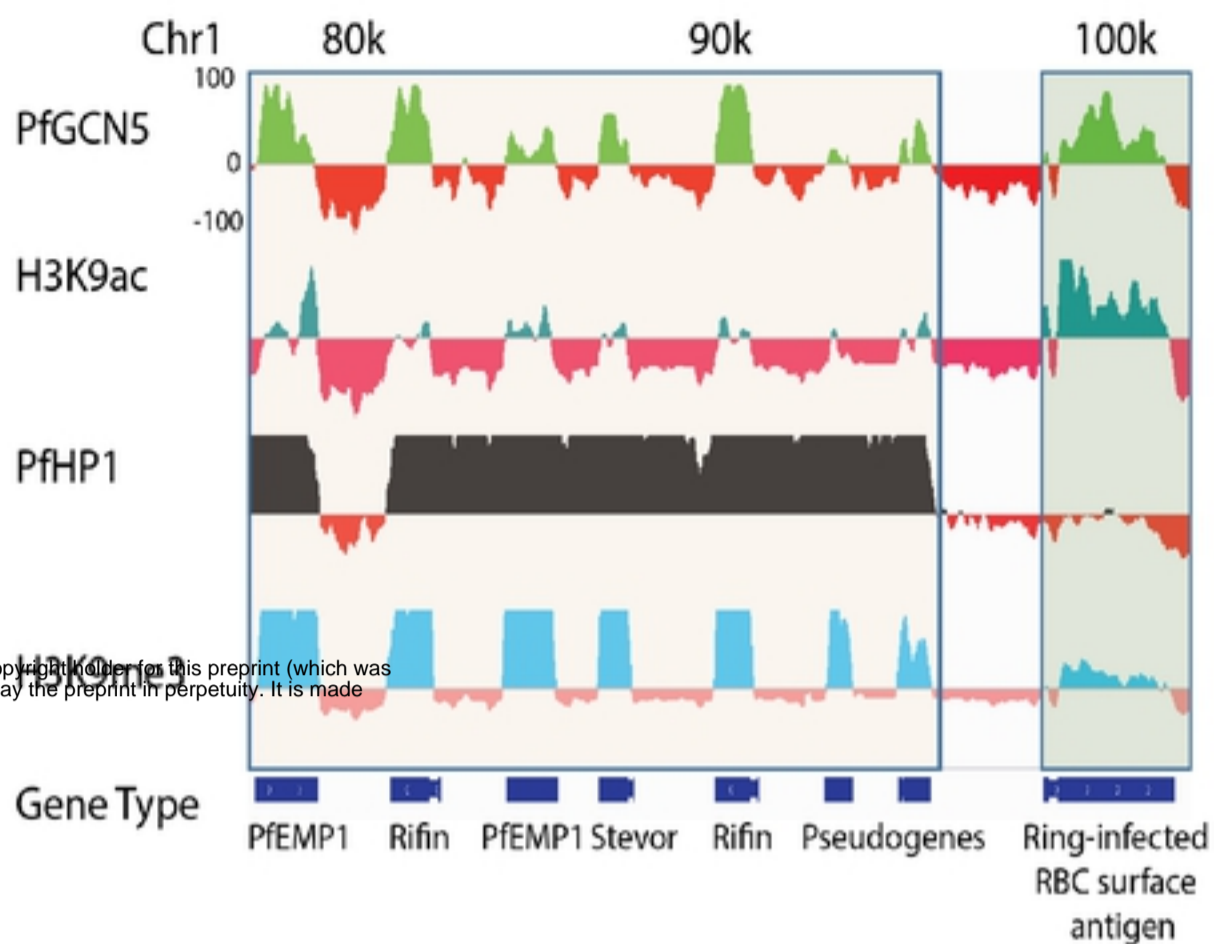
1104 **Supplementary Figure S6: PfGCN5 regulates antigenic variation and stress response**
1105 **machinery in artemisinin resistant strains of Plasmodium.** (S6A) Venn diagram showing
1106 the genes bound by PfGCN5 in K13-I543T (MRA-1241) and K13-C580Y (MRA-1236)
1107 mutant lines and their sensitive counterpart K13-I543wt (MRA-1253) and K13-C580wt
1108 (MRA-1254) respectively. Genes associated with antigenic variation and cellular adhesions
1109 were found to be core targets of PfGCN5 in both sensitive and resistant strains. Unique set of
1110 genes implicated in resistance in the field were enriched for PfGCN5 occupancy in the two
1111 resistant strains. (S6B) Venn-diagram showing the overlap between the various proteins
1112 which were pulled down during PfGCN5 immunoprecipitation and the protein found in the
1113 vesicles secreted by the artemisinin resistant parasites.

Figure 1

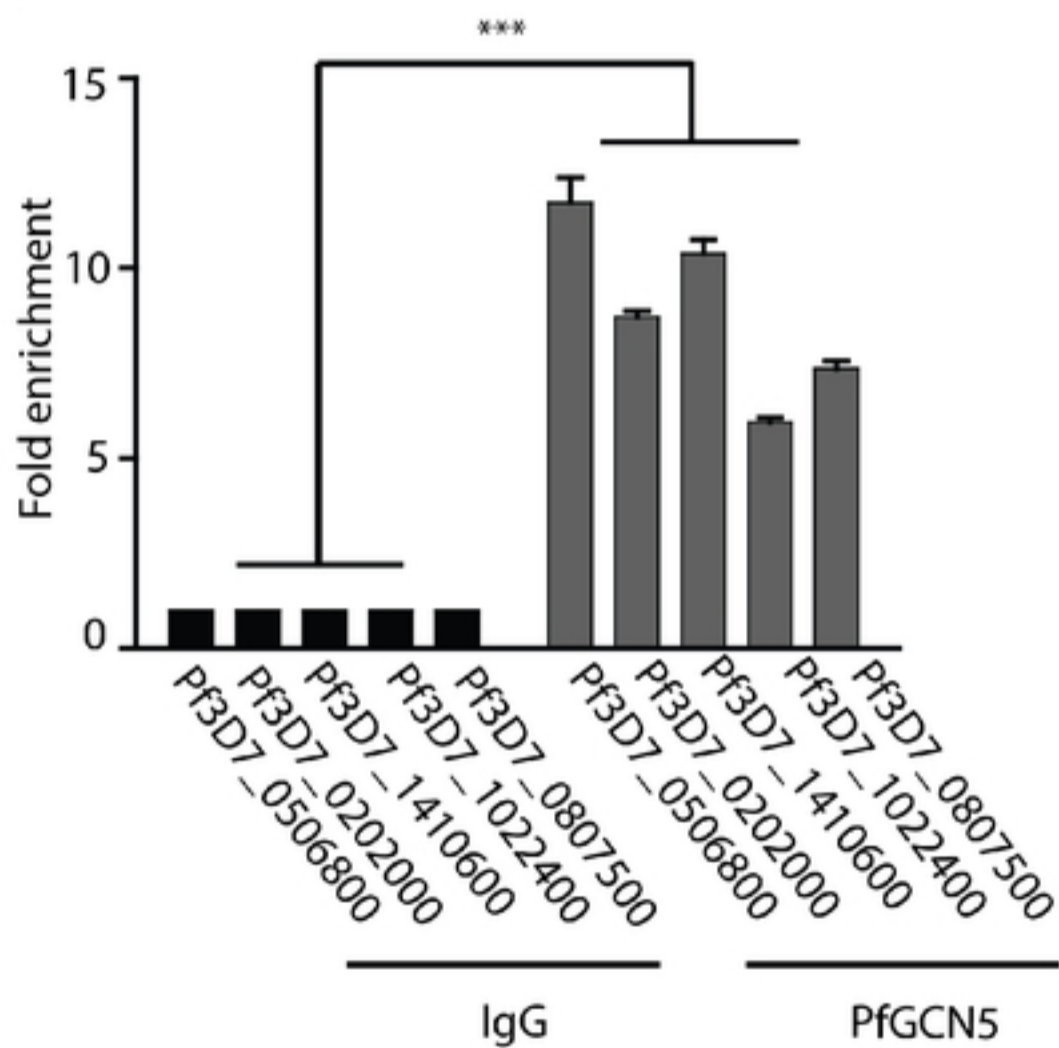
1A



1B



1C



1D

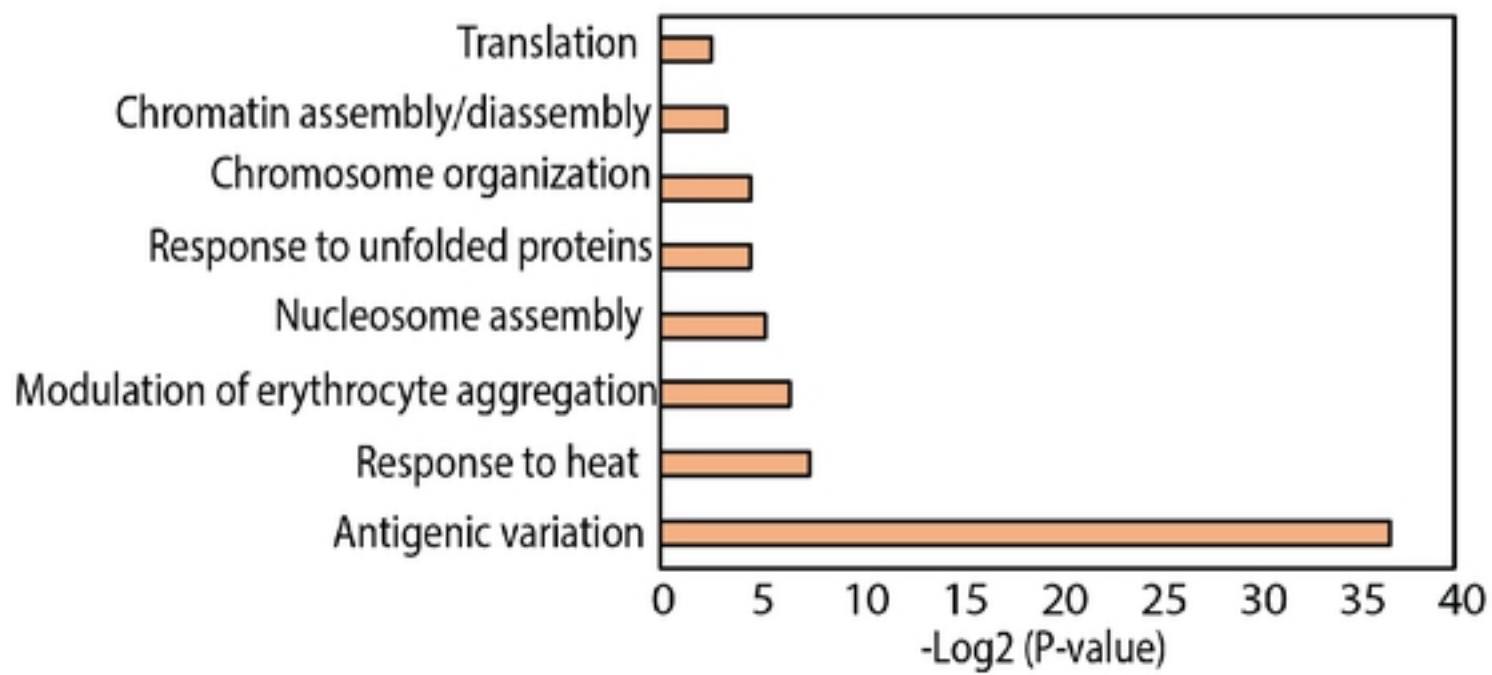
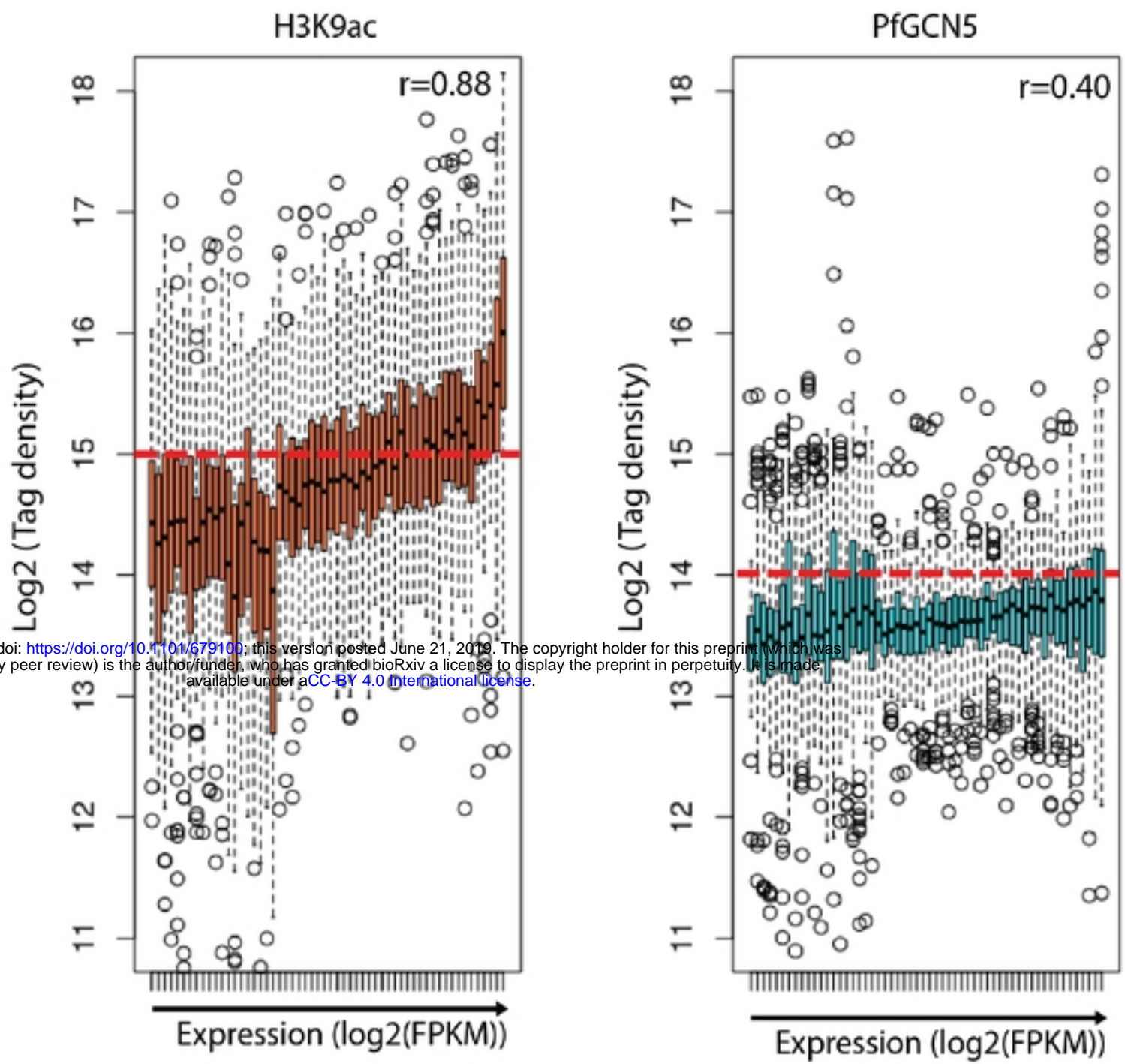


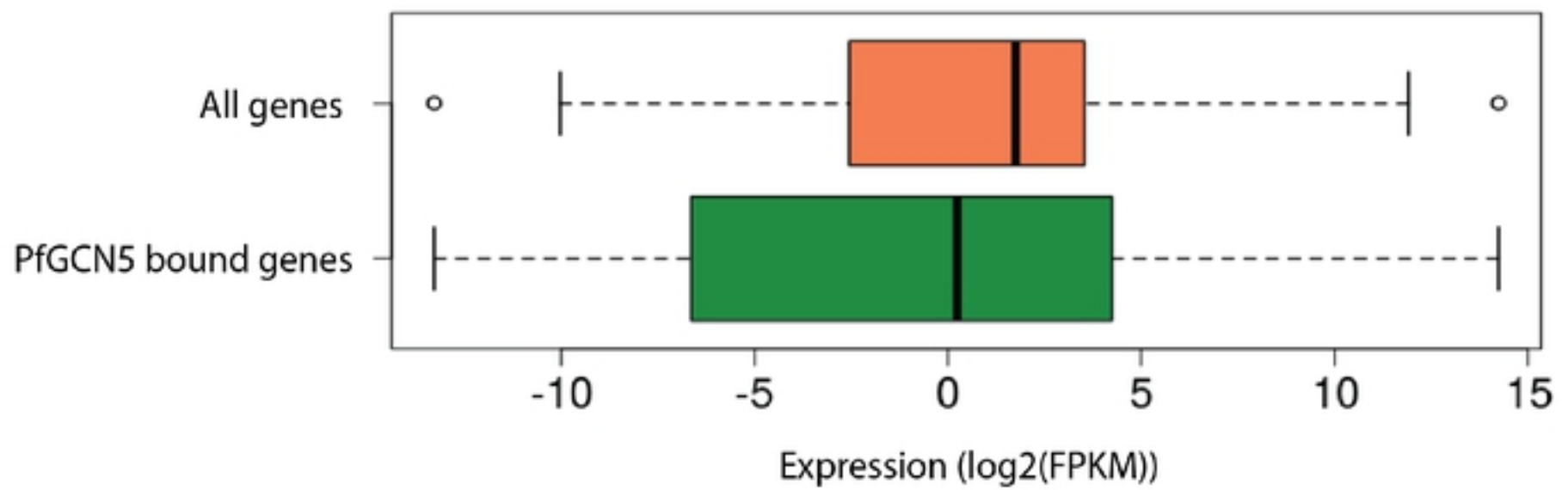
Figure 2

2A

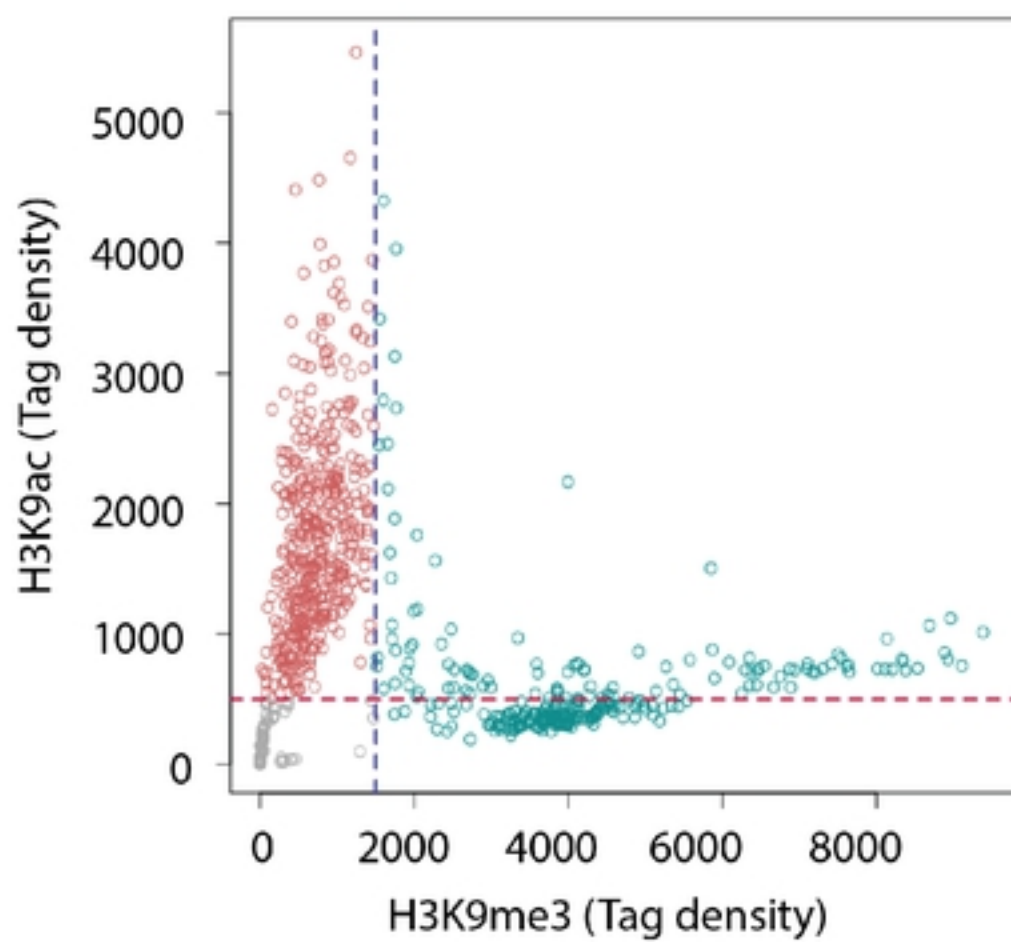


bioRxiv preprint doi: <https://doi.org/10.1101/679100>; this version posted June 21, 2019. The copyright holder for this preprint (which was not certified by peer review) is the author/funder, who has granted bioRxiv a license to display the preprint in perpetuity. It is made available under aCC-BY 4.0 International license.

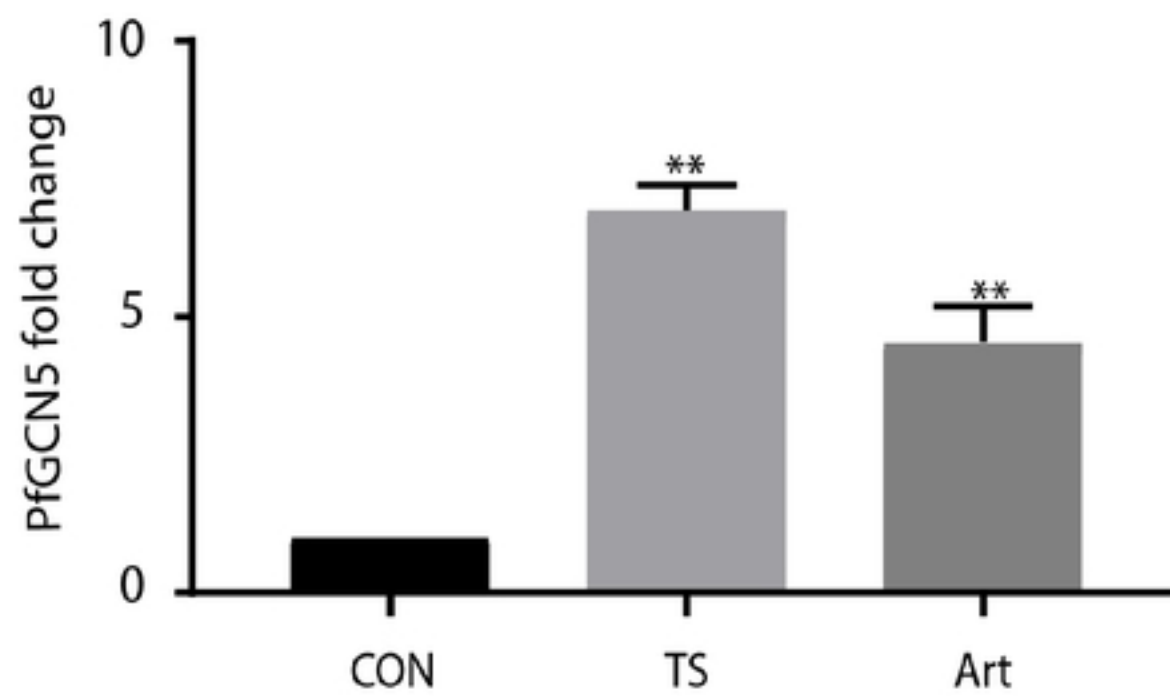
2B



2C

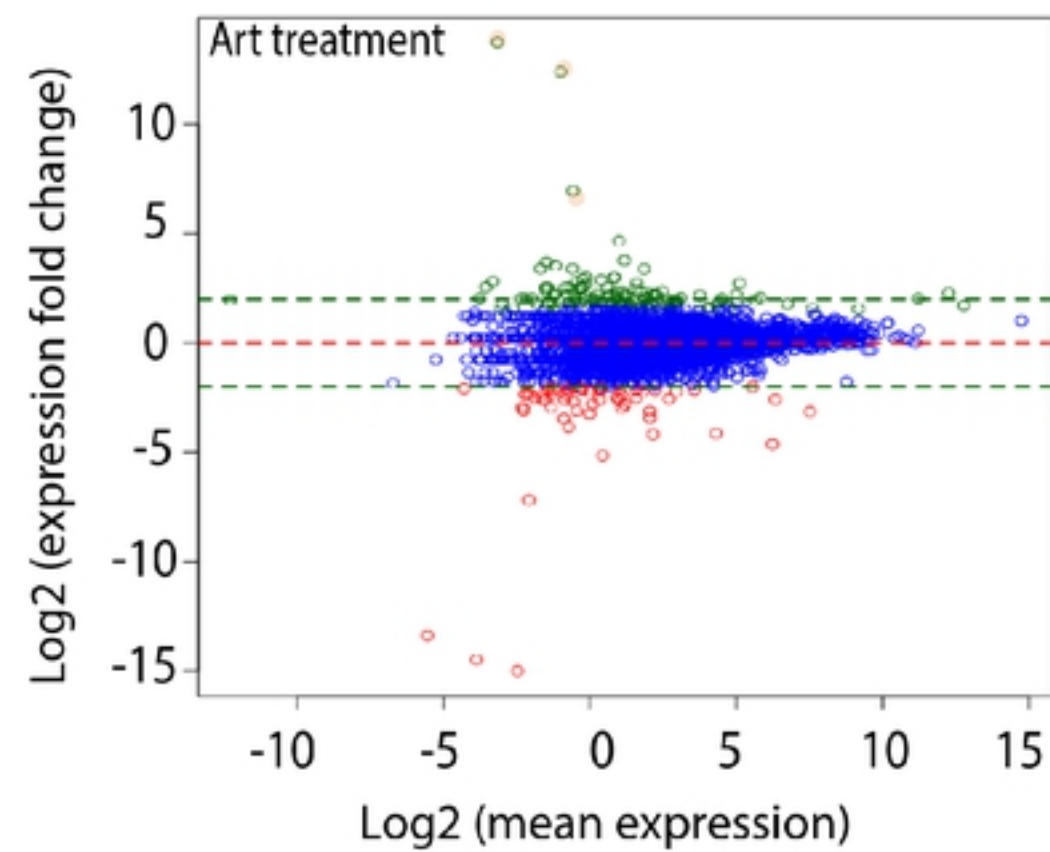


3A

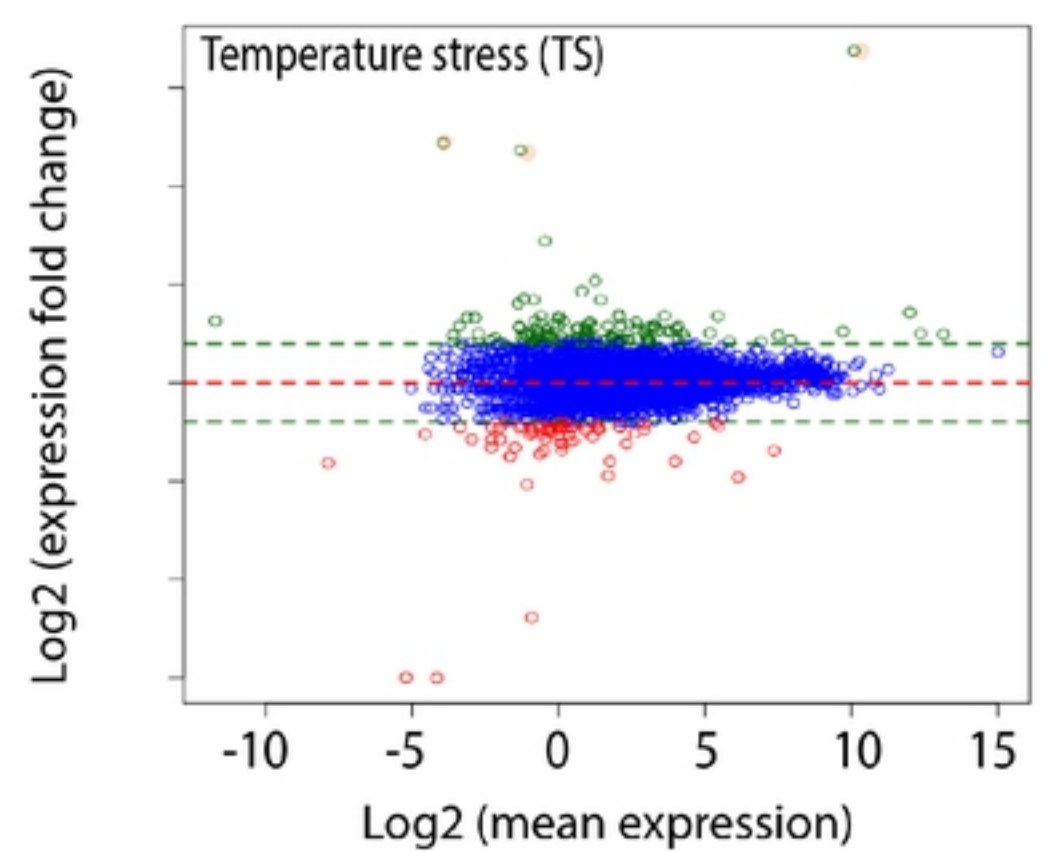


bioRxiv preprint doi: <https://doi.org/10.1101/679100>; this version posted June 21, 2019. The copyright holder for this preprint (which was not certified by peer review) is the author/funder, who has granted bioRxiv a license to display the preprint in perpetuity. It is made available under aCC-BY 4.0 International license.

3B



3C



3D

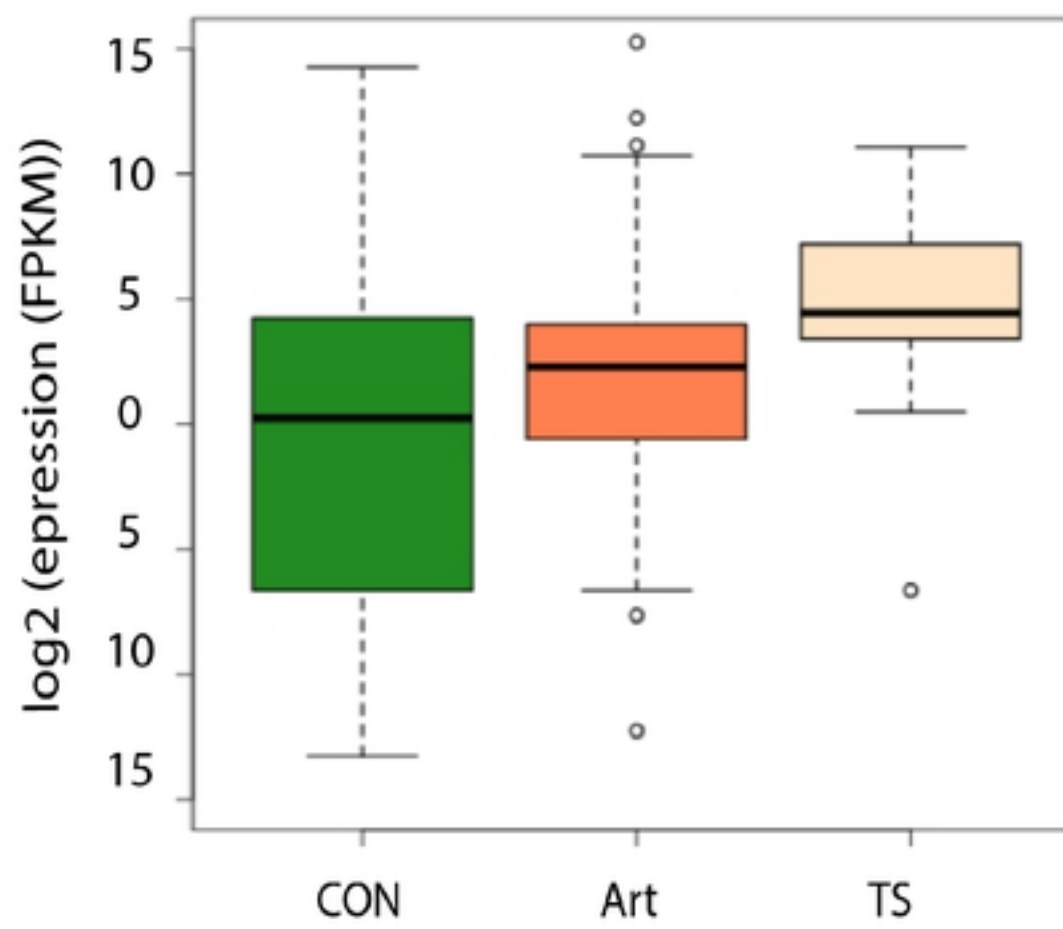
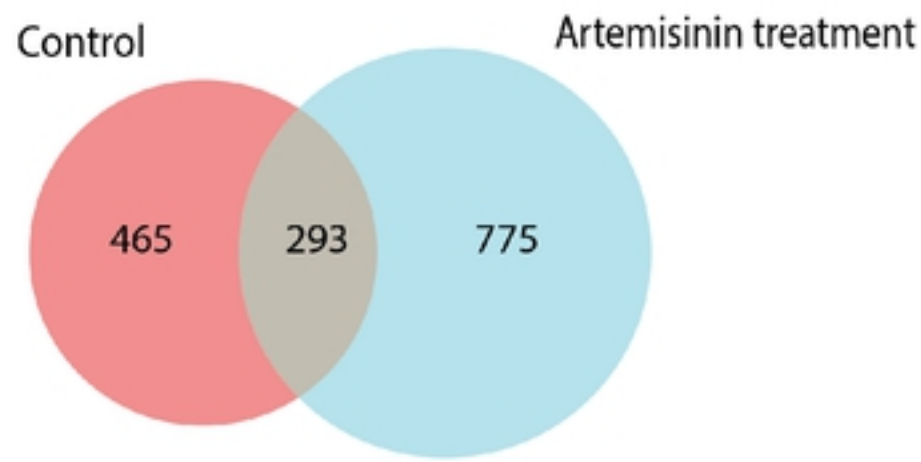
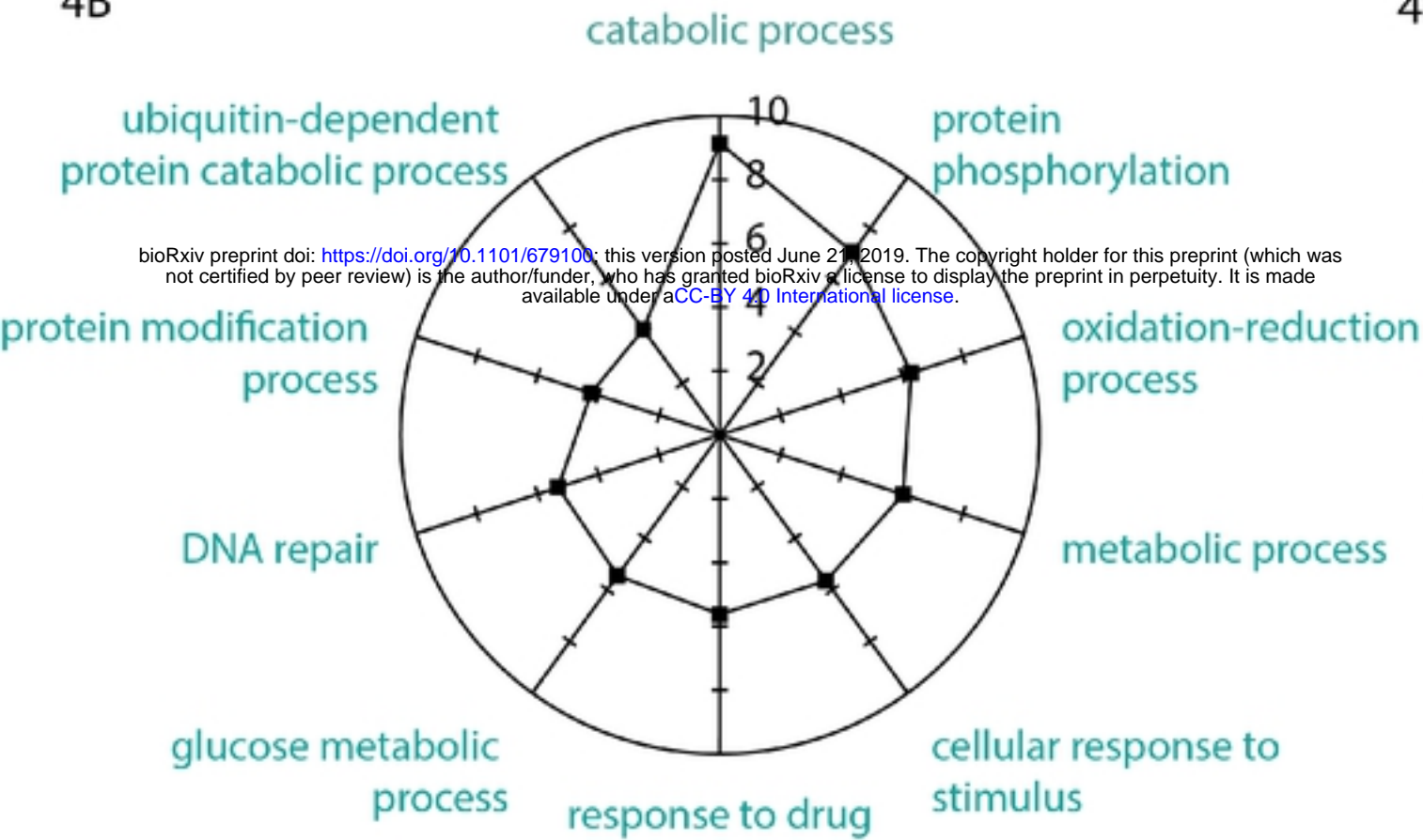


Figure 4

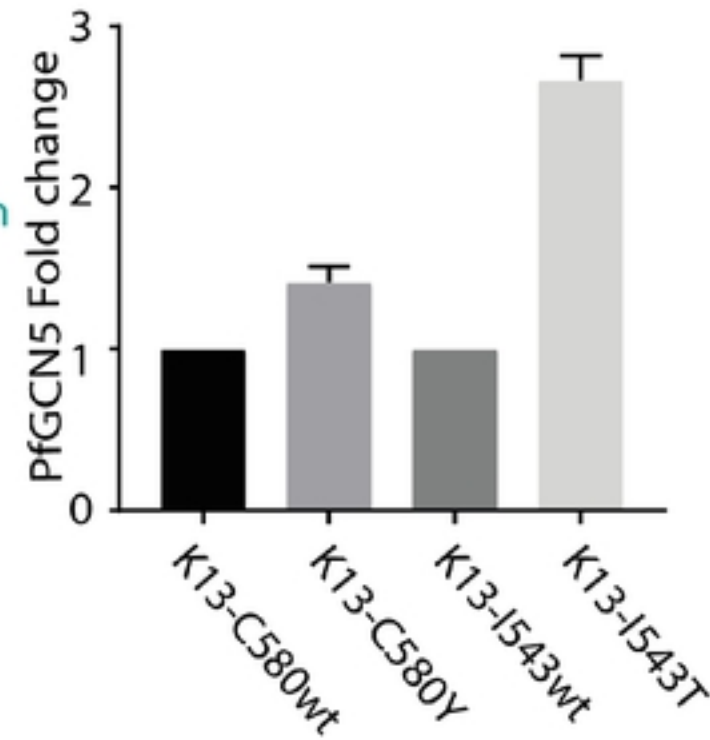
4A



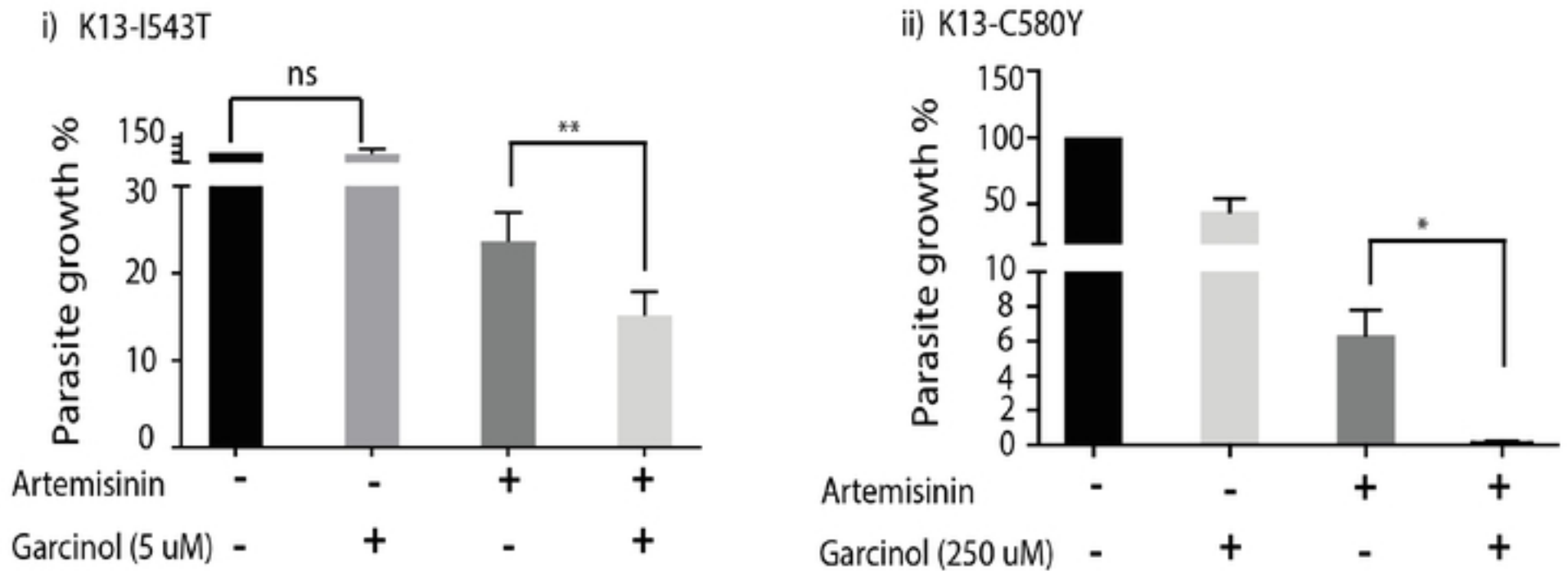
4B



4C



4D



4E

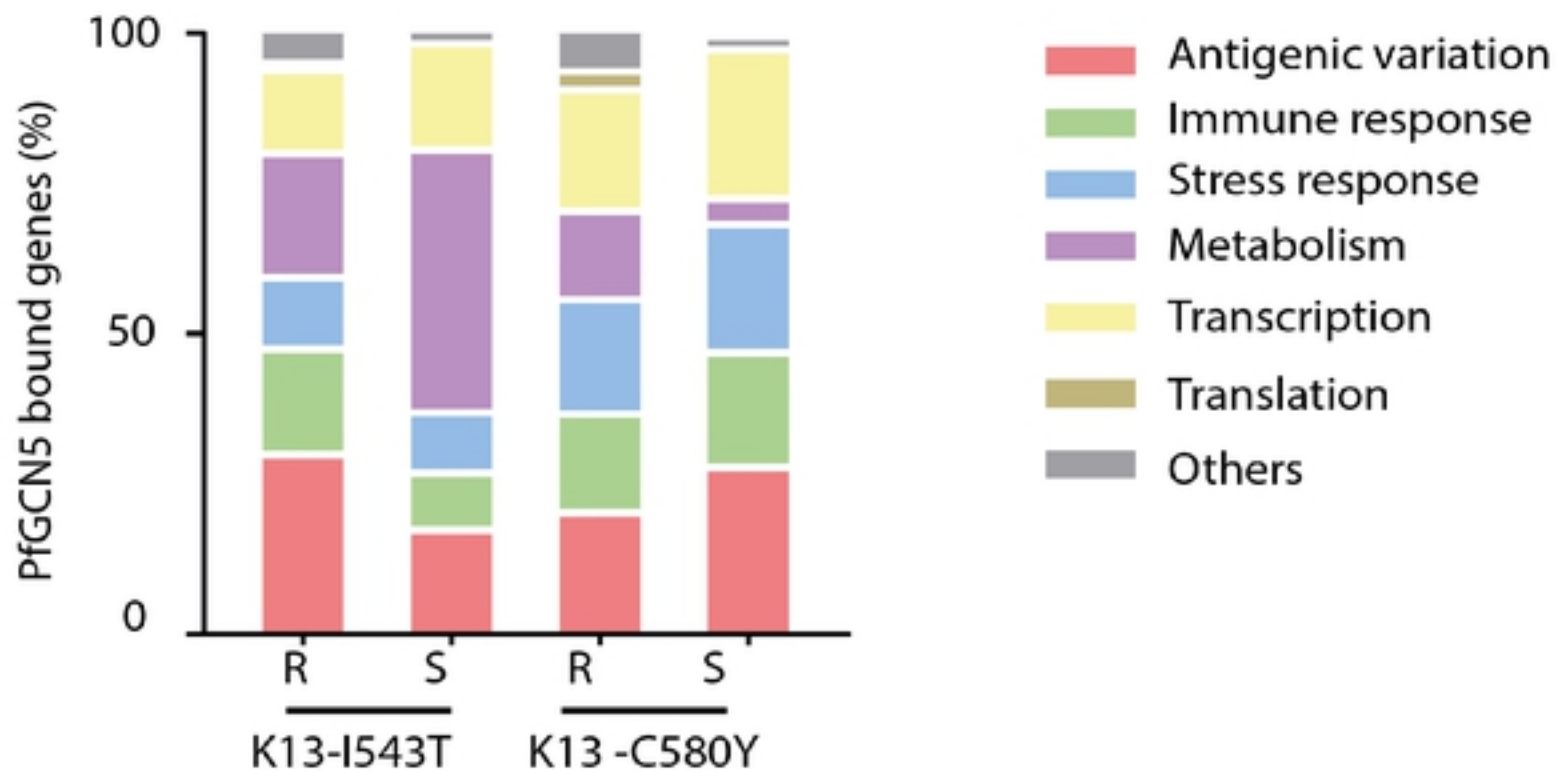
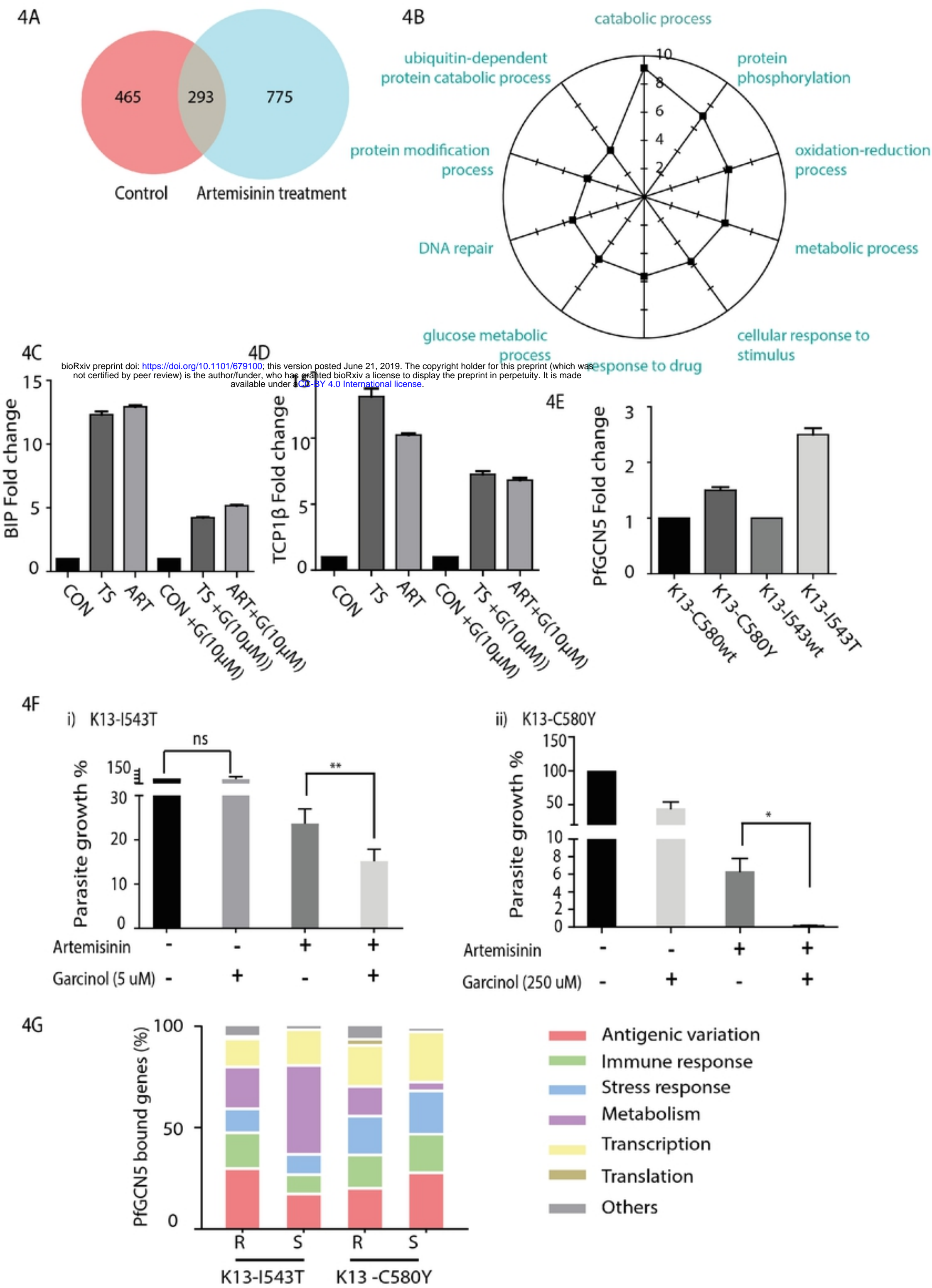


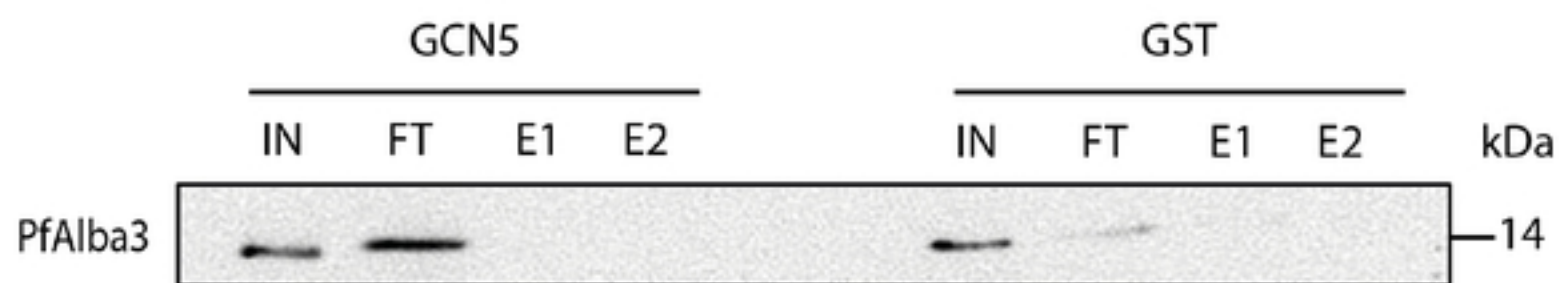
Figure 4



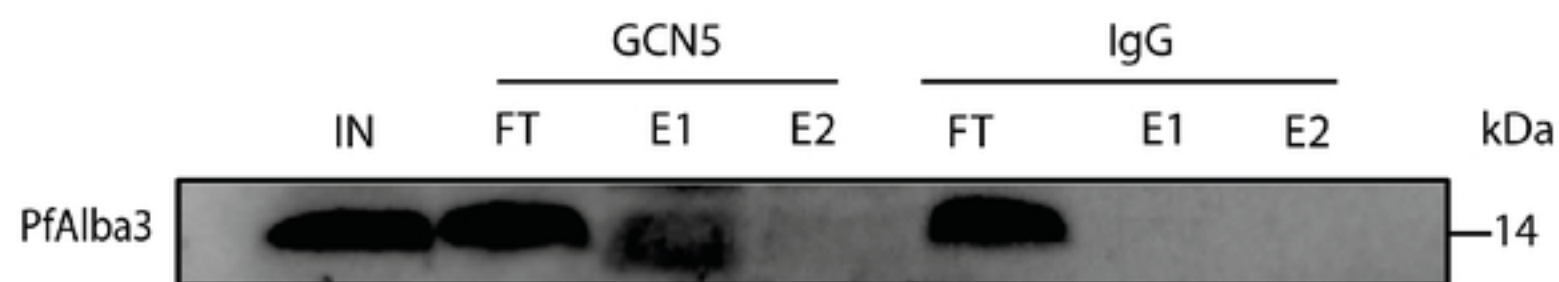
bioRxiv preprint doi: <https://doi.org/10.1101/679100>; this version posted June 21, 2019. The copyright holder for this preprint (which was not certified by peer review) is the author/funder, who has granted bioRxiv a license to display the preprint in perpetuity. It is made available under aCC-BY 4.0 International license.

Figure 5

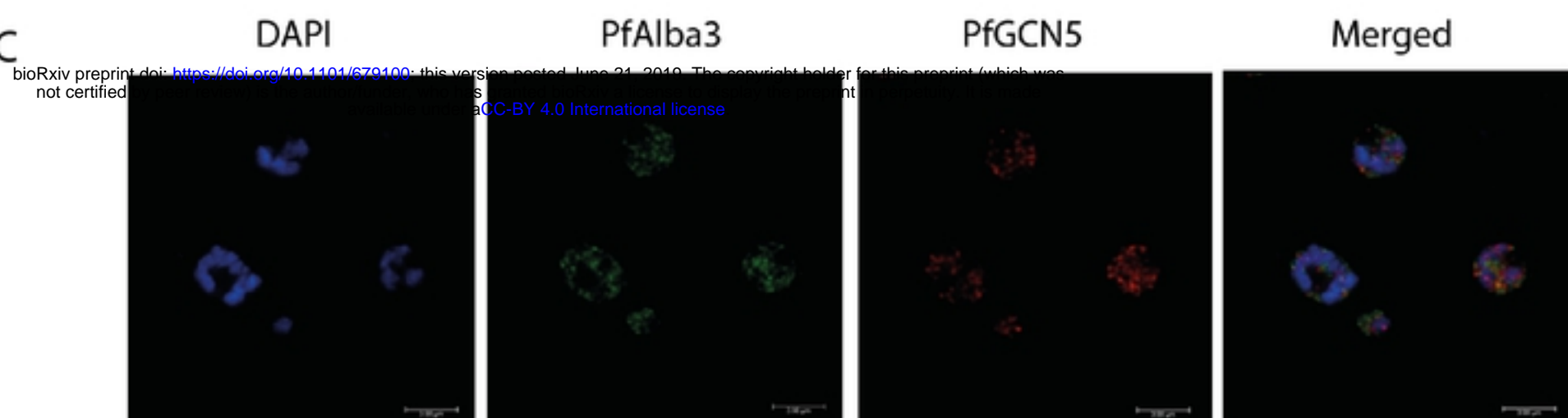
5A



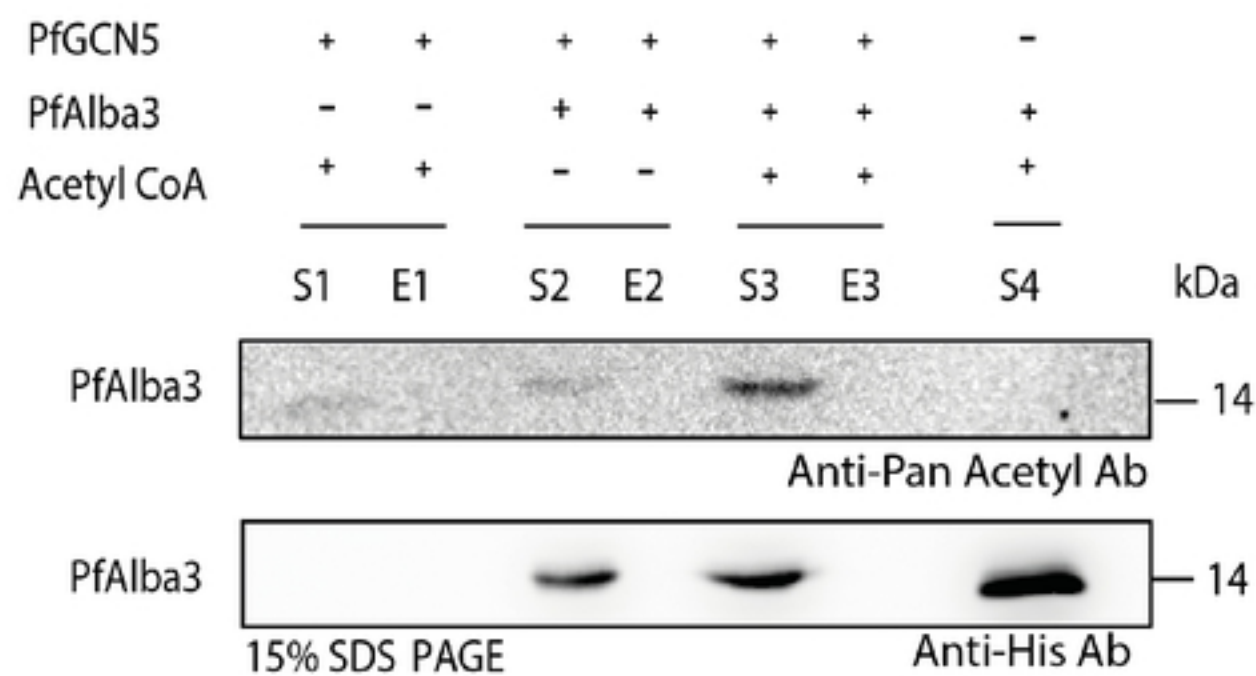
5B



5C



5D



5E

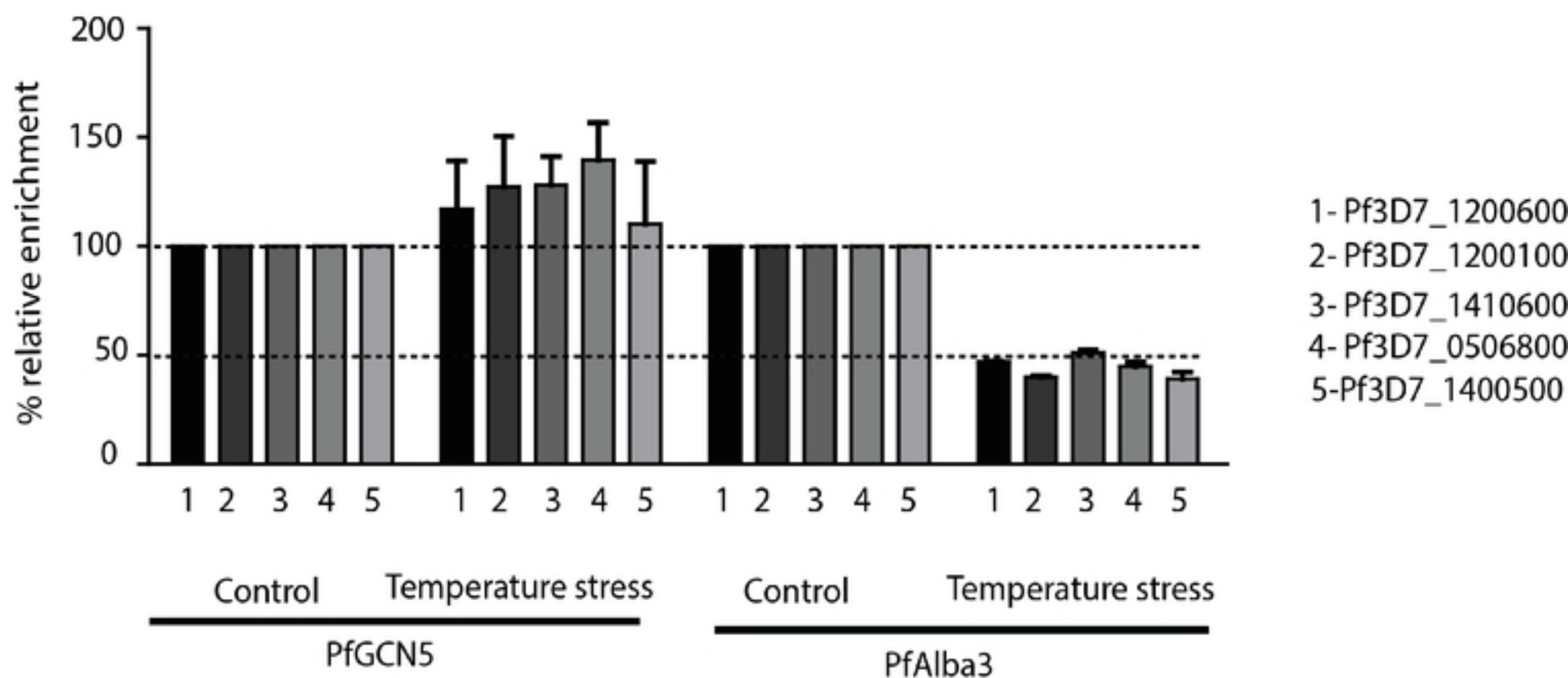
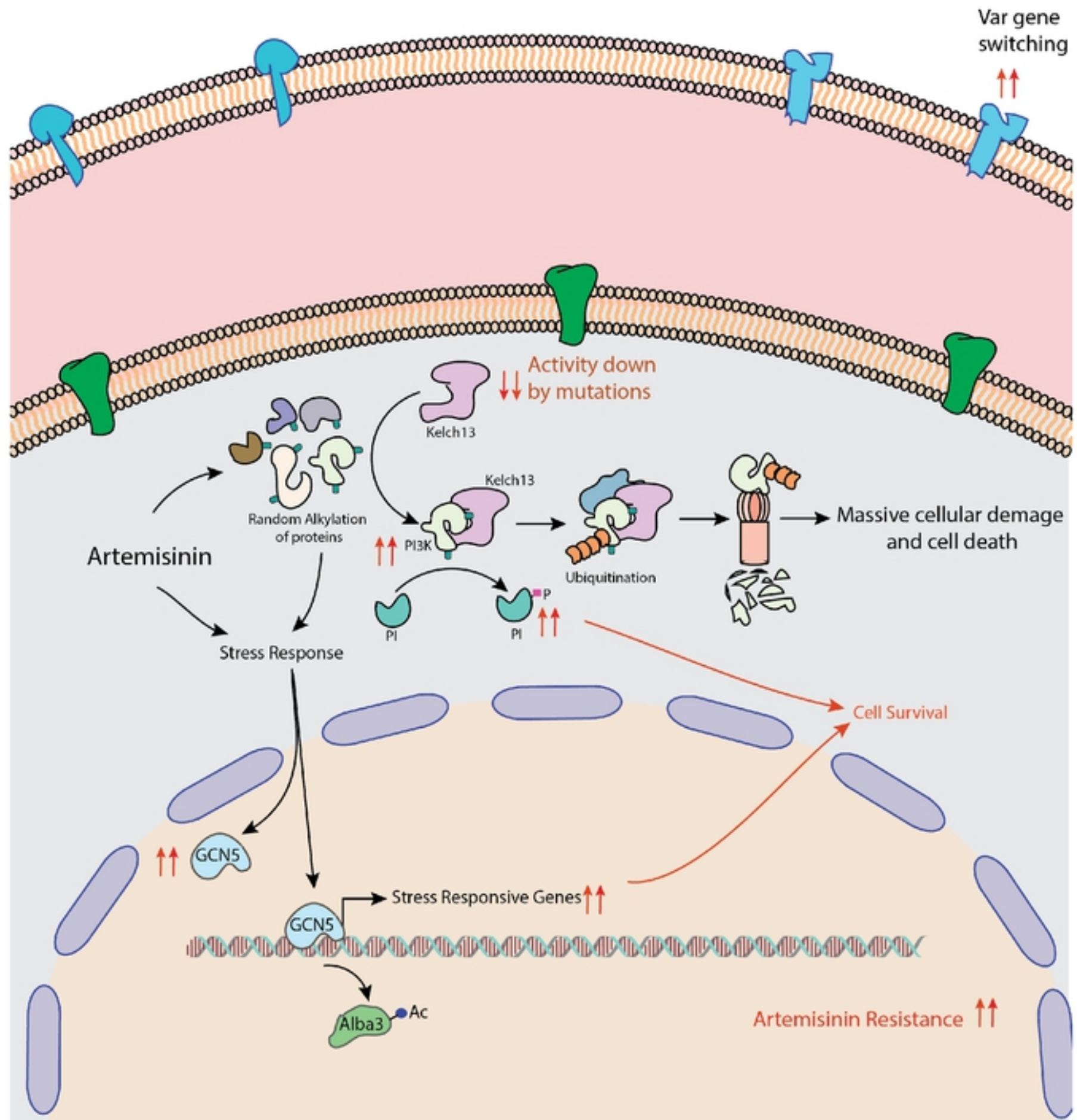


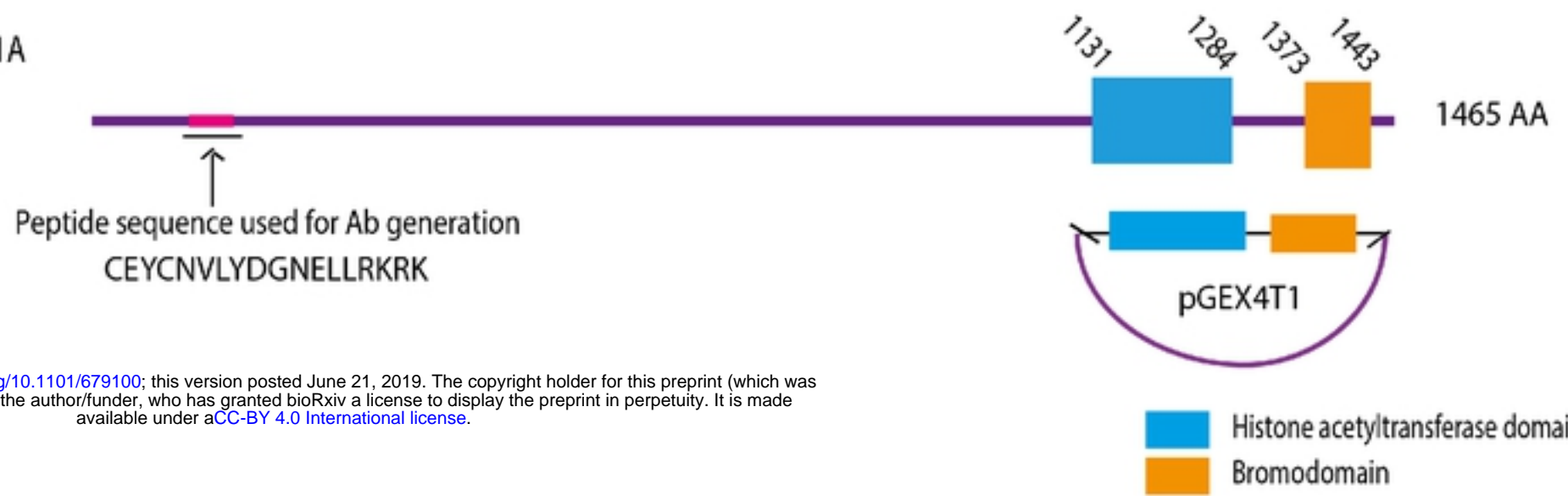
Figure 6

bioRxiv preprint doi: <https://doi.org/10.1101/679100>; this version posted June 21, 2019. The copyright holder for this preprint (which was not certified by peer review) is the author/funder, who has granted bioRxiv a license to display the preprint in perpetuity. It is made available under aCC-BY 4.0 International license.



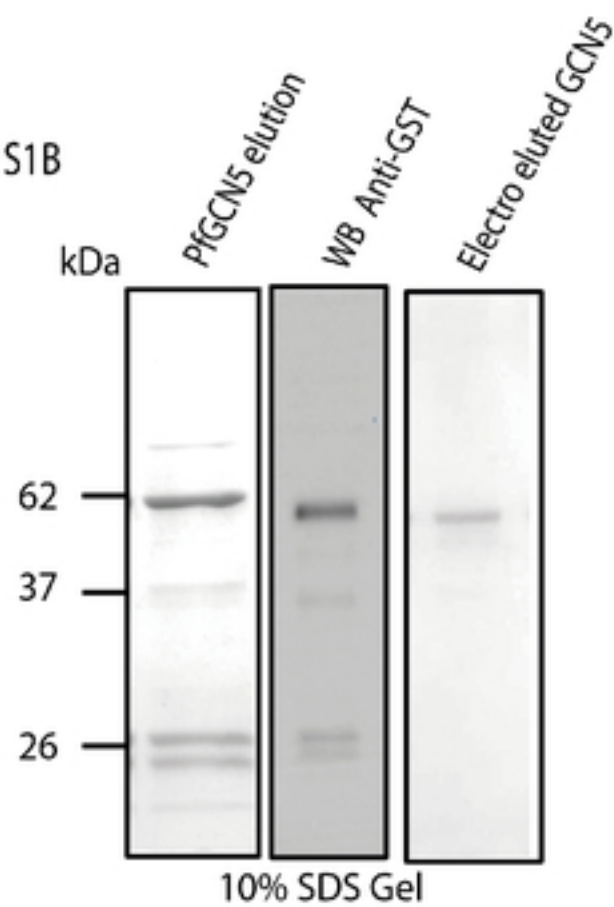
Supplementary Figure S1

S1A

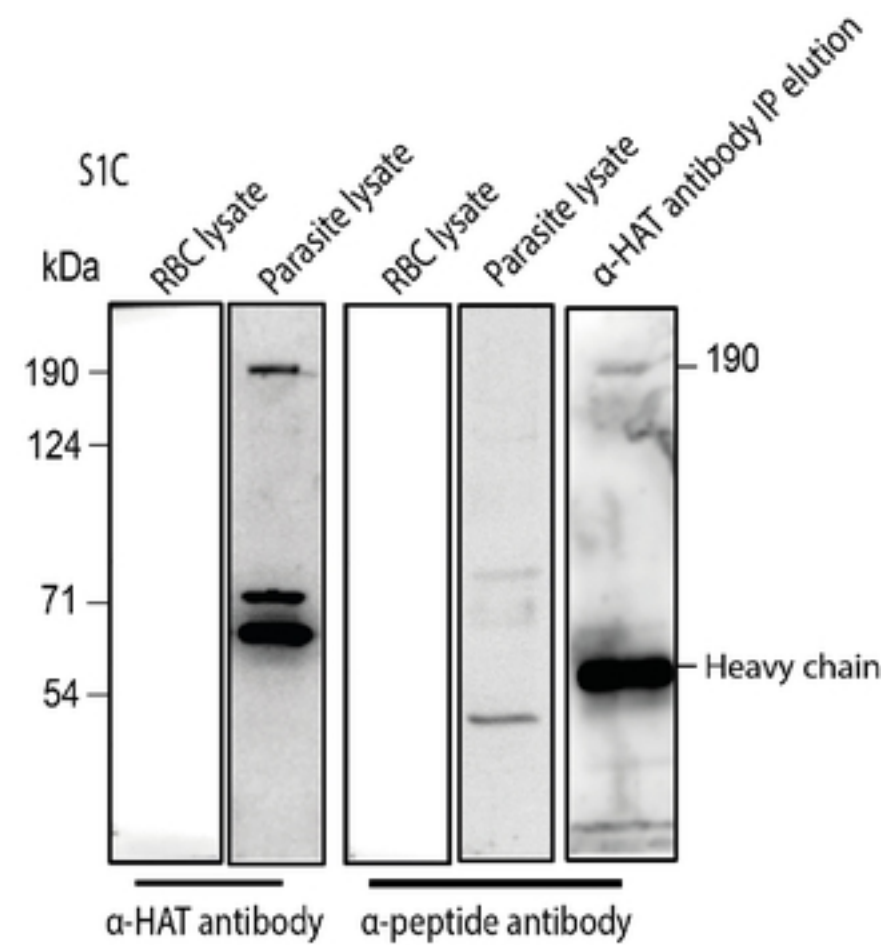


bioRxiv preprint doi: <https://doi.org/10.1101/679100>; this version posted June 21, 2019. The copyright holder for this preprint (which was not certified by peer review) is the author/funder, who has granted bioRxiv a license to display the preprint in perpetuity. It is made available under aCC-BY 4.0 International license.

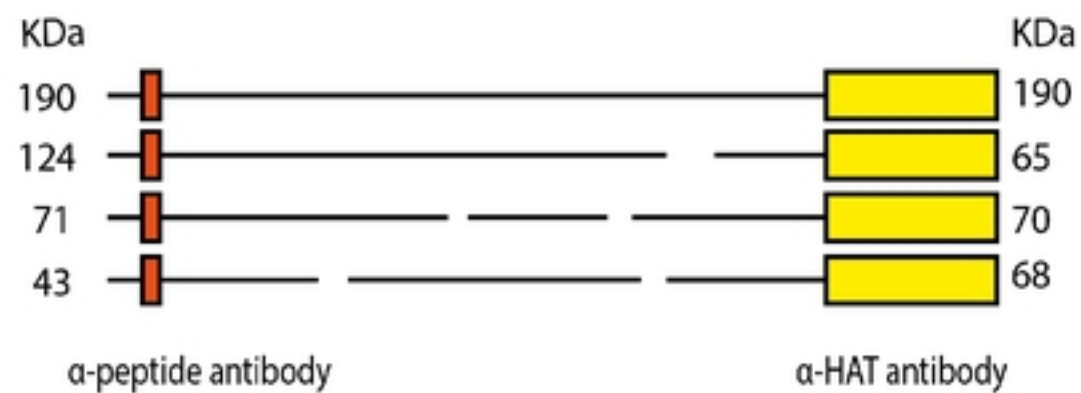
S1B



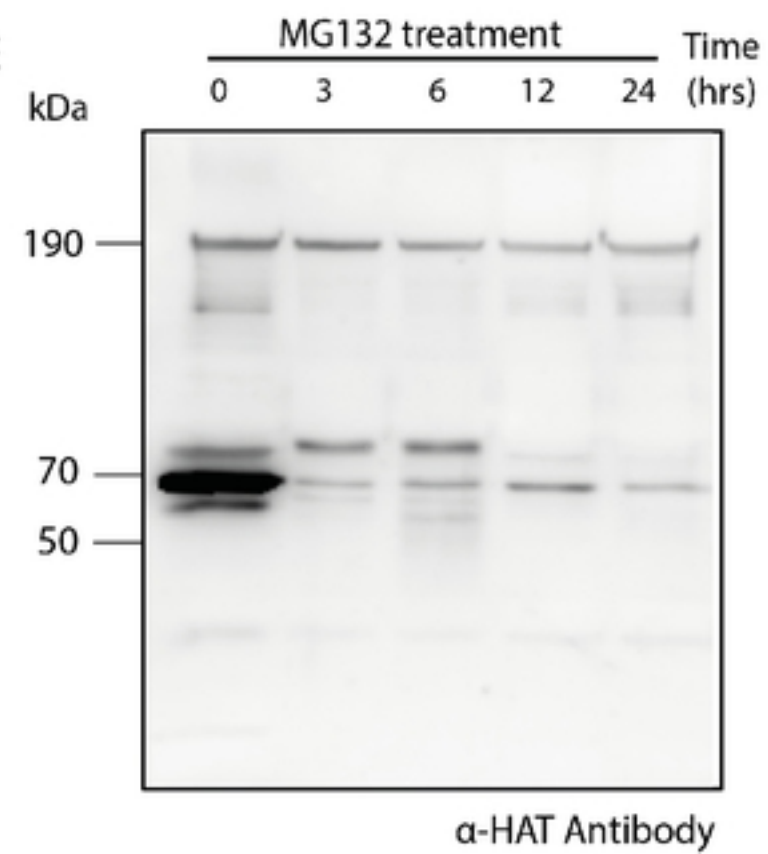
S1C



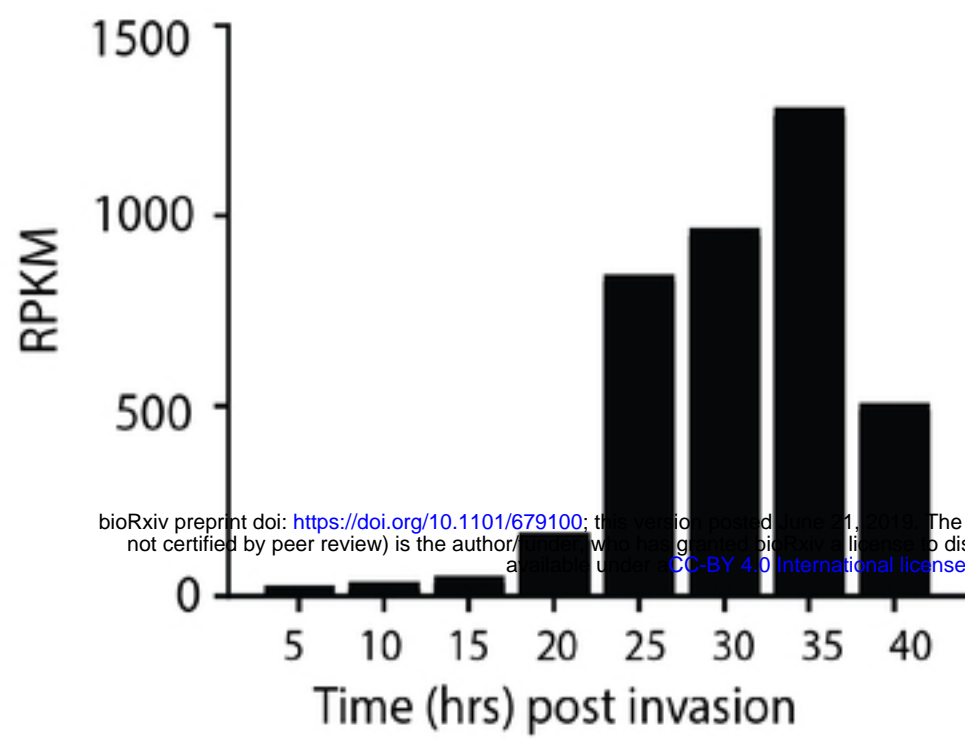
S1D



S1E

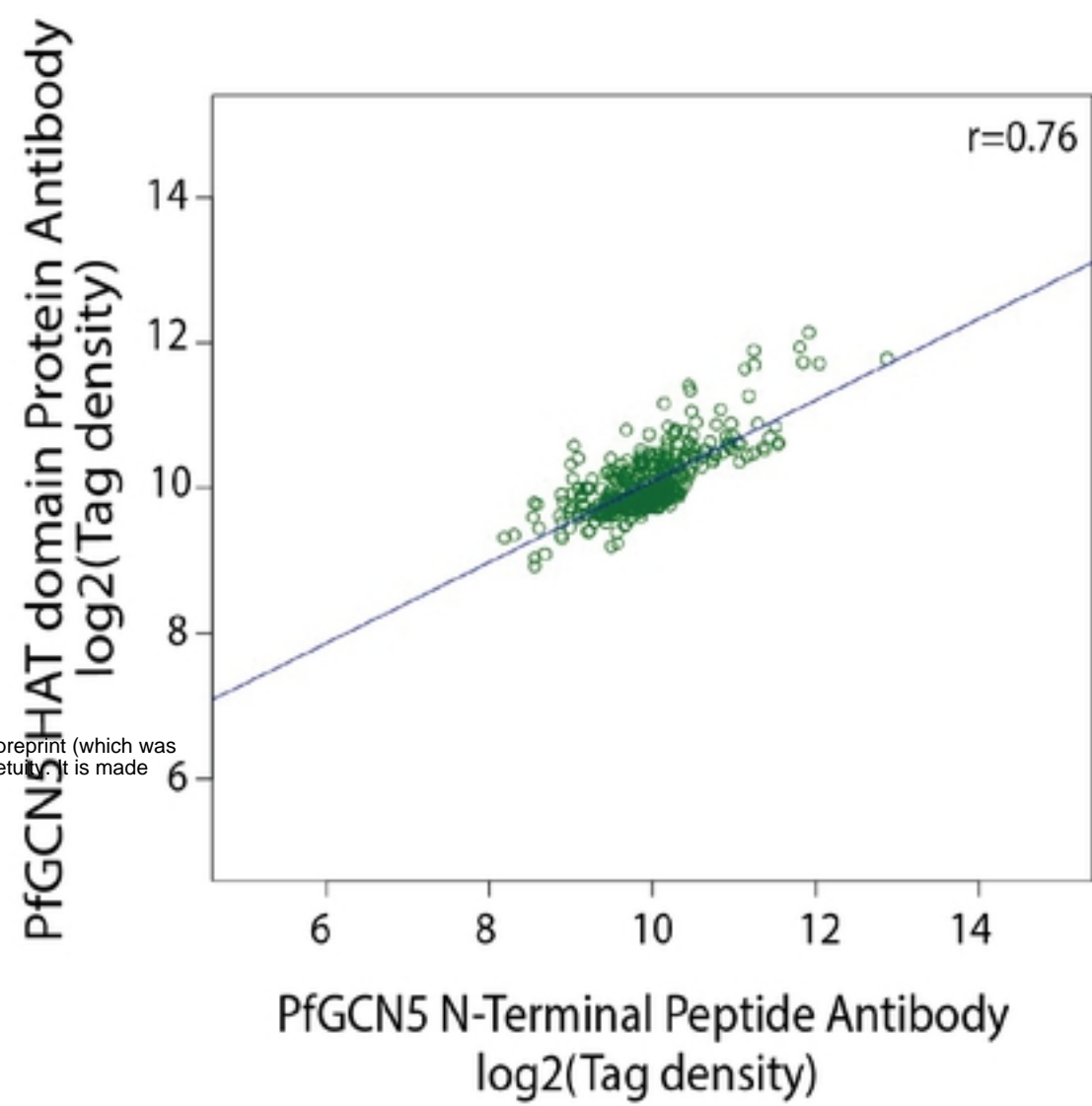


S2A

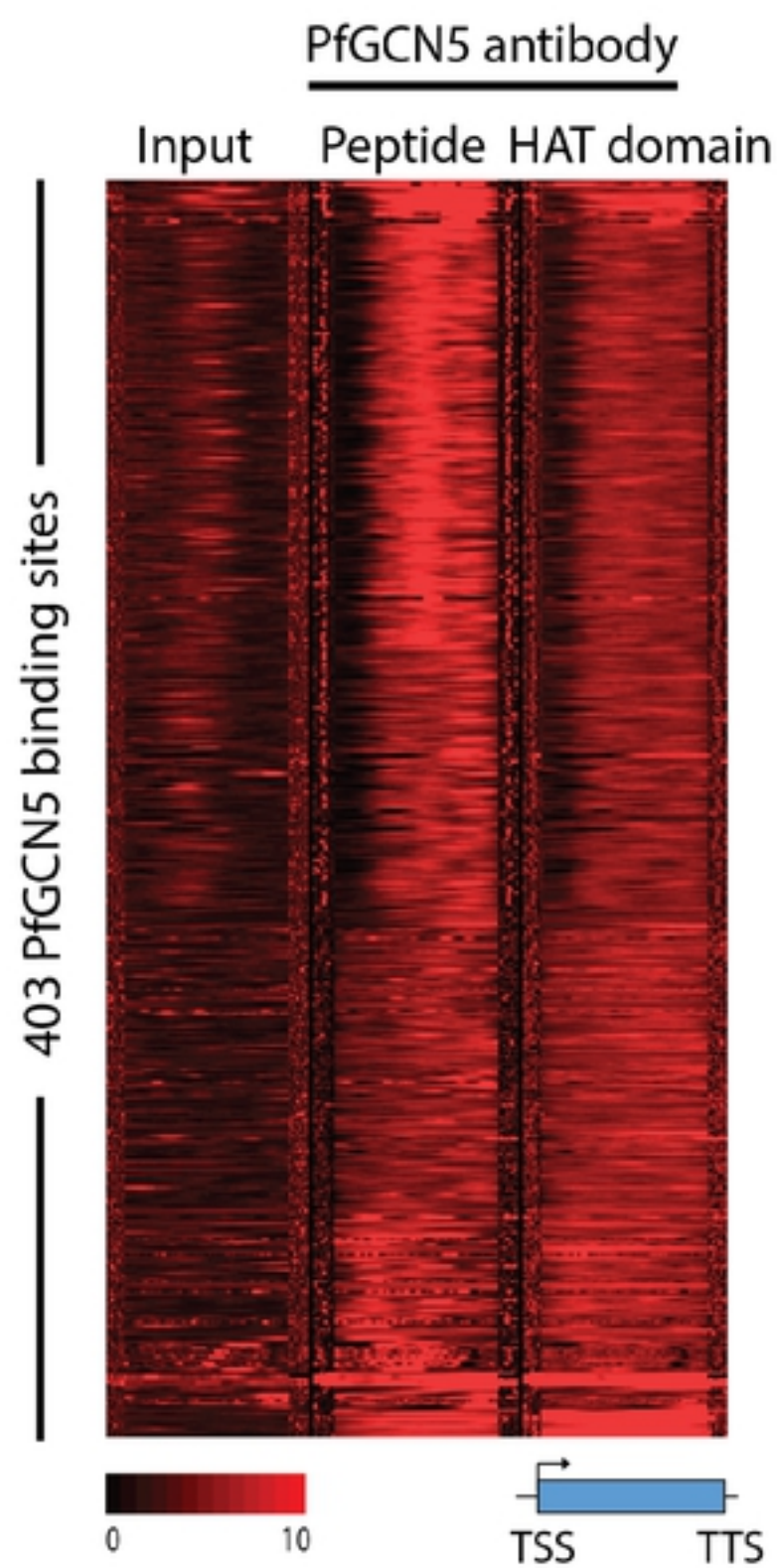


bioRxiv preprint doi: <https://doi.org/10.1101/679100>; this version posted August 1, 2020. The copyright holder for this preprint (which was not certified by peer review) is the author/funder, who has granted bioRxiv a license to display the preprint in perpetuity. It is made available under aCC-BY 4.0 International license.

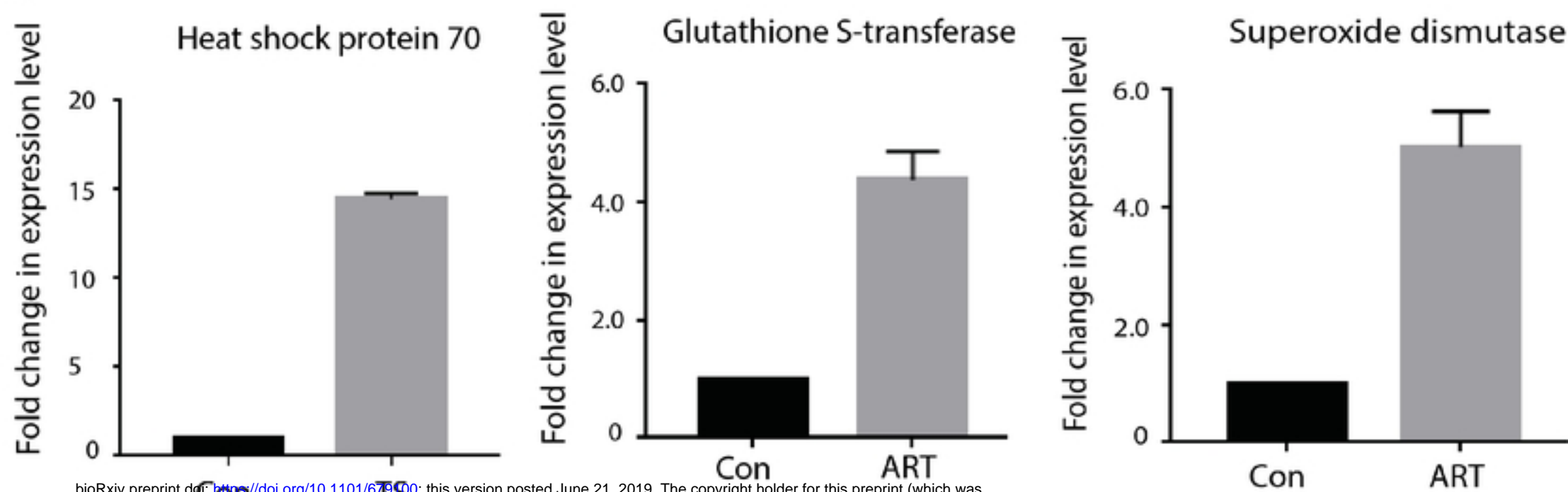
S2B



S2C

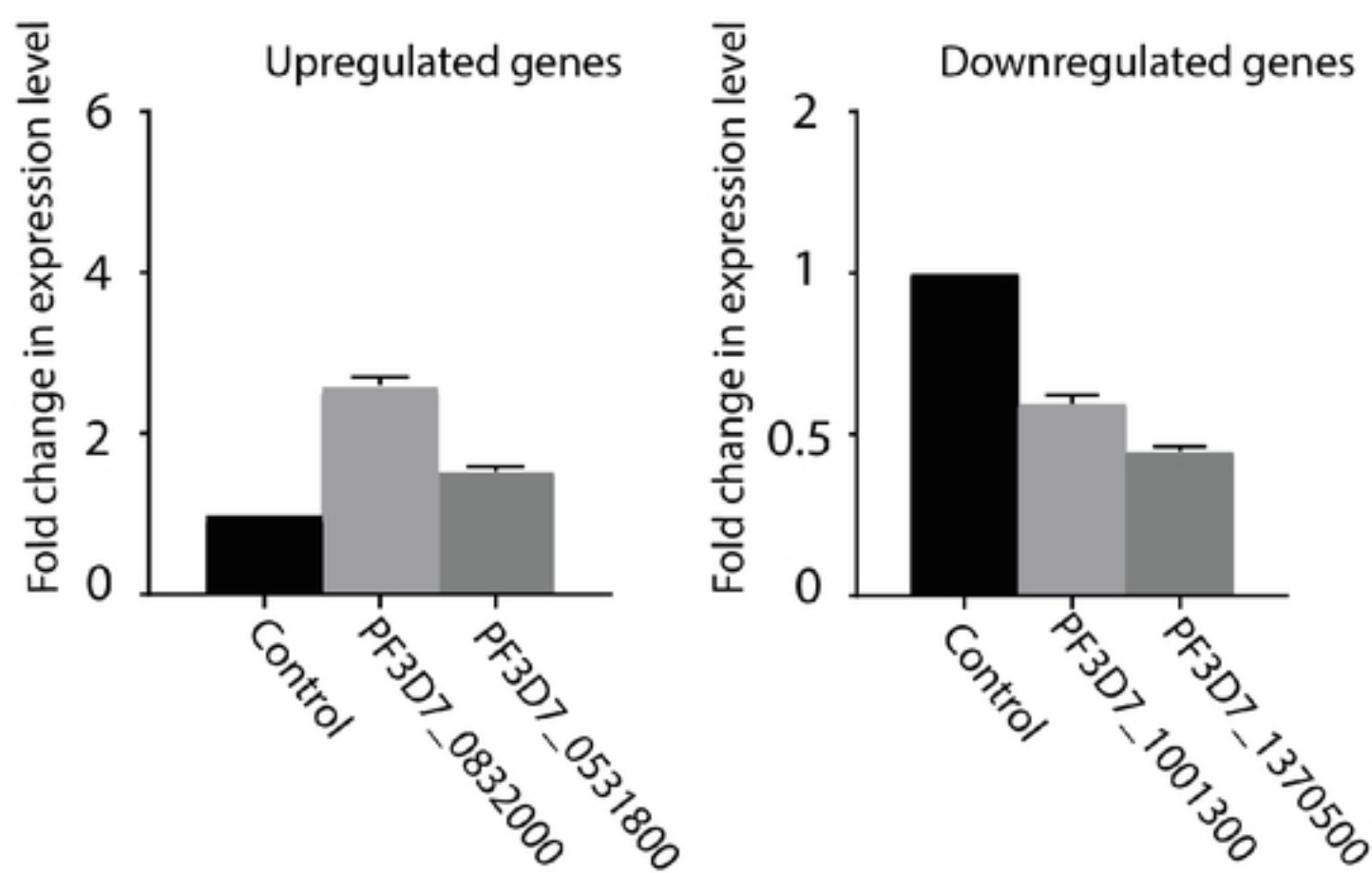


S3A

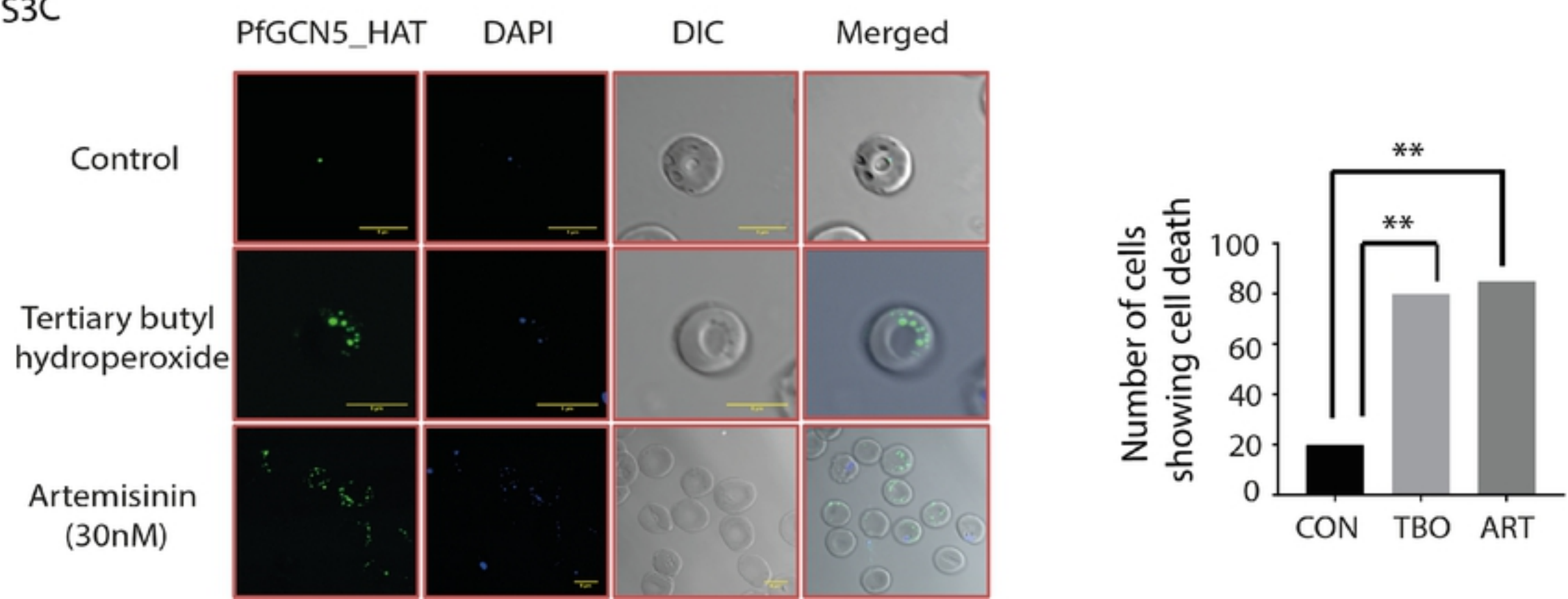


bioRxiv preprint doi: <https://doi.org/10.1101/679400>; this version posted June 21, 2019. The copyright holder for this preprint (which was not certified by peer review) is the author/funder, who has granted bioRxiv a license to display the preprint in perpetuity. It is made available under aCC-BY 4.0 International license.

S3B

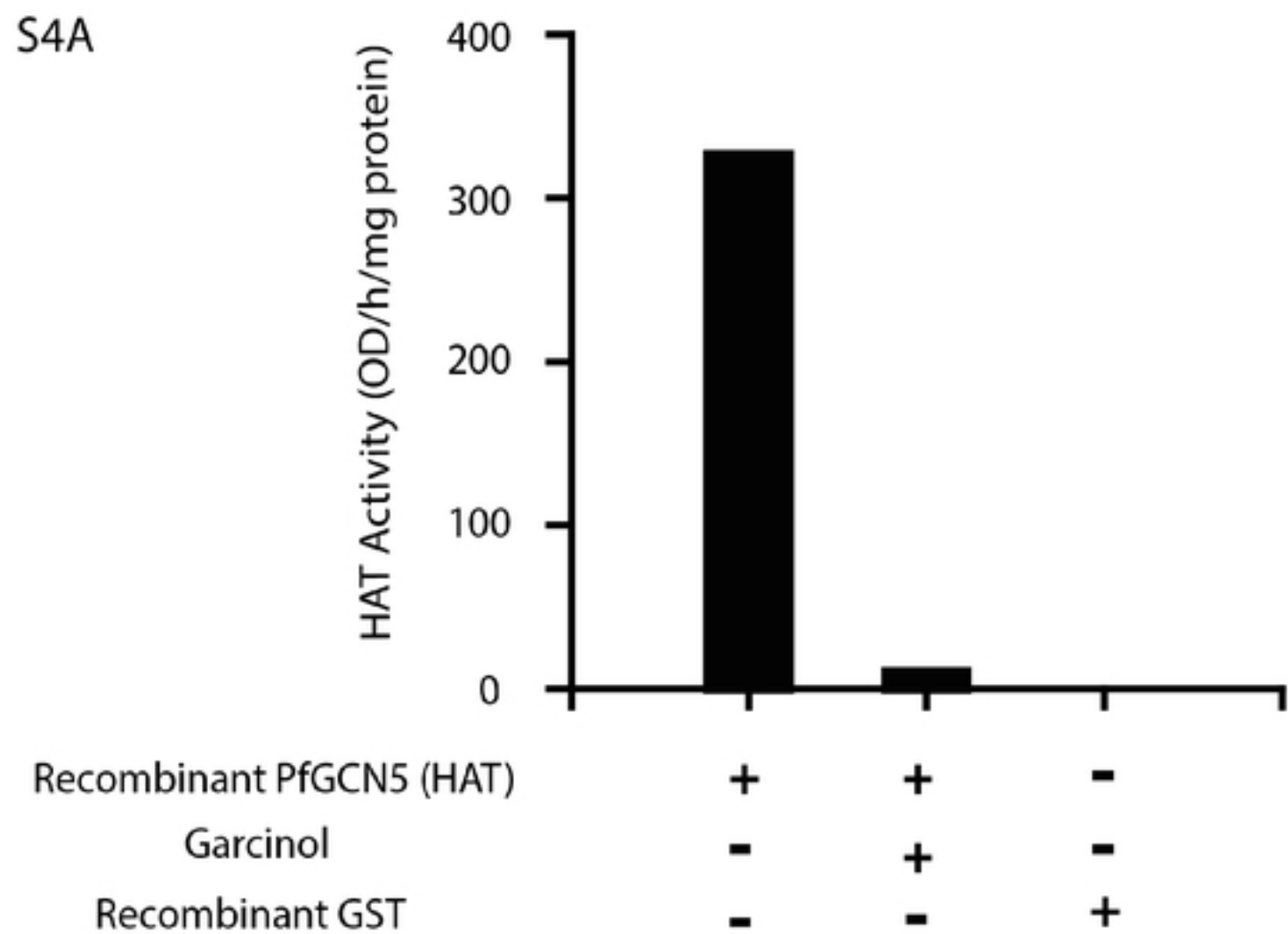


S3C



Supplementary Figure S4

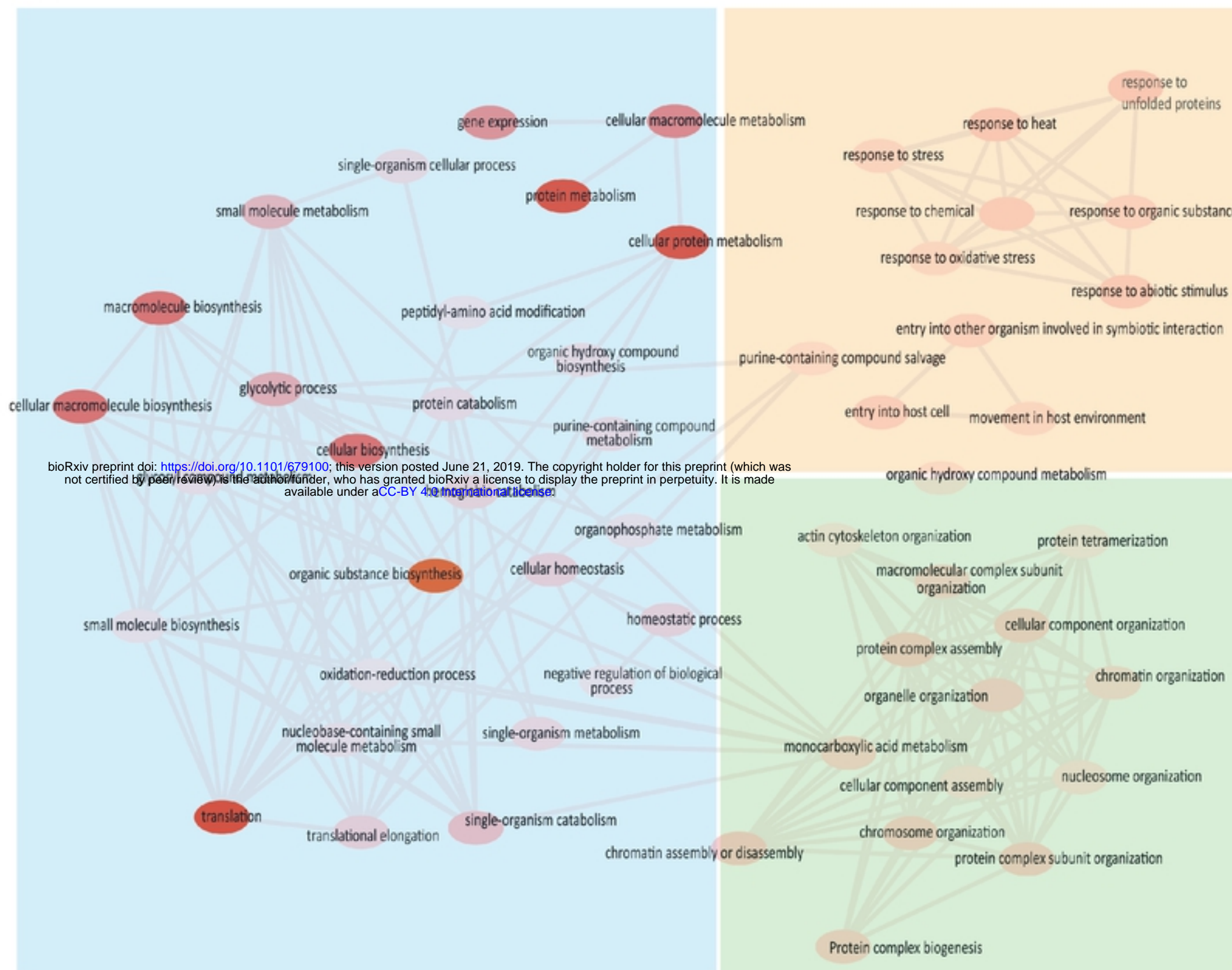
bioRxiv preprint doi: <https://doi.org/10.1101/679100>; this version posted June 21, 2019. The copyright holder for this preprint (which was not certified by peer review) is the author/funder, who has granted bioRxiv a license to display the preprint in perpetuity. It is made available under aCC-BY 4.0 International license.



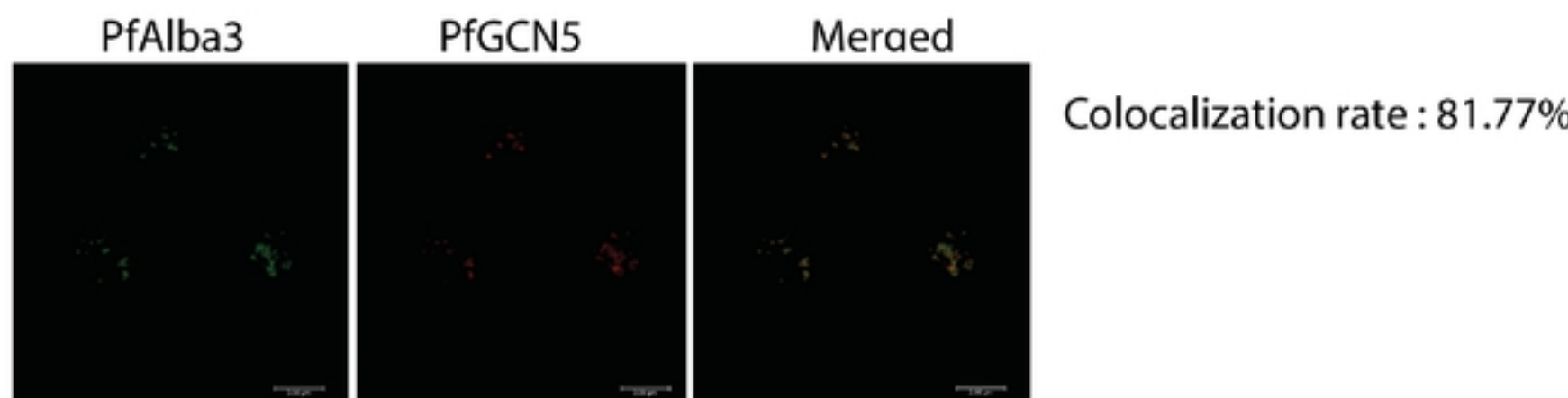
S4B

	Estimation	Standard error	Lower CI95%	UpperCI95%	Ration CI
IC50	15	3.58	6.75	23.25	3.45
IC90	18.69	4.46	8.41	28.97	3.45
IC99	23.75	5.67	10.68	36.82	3.45
Gamma	10	-	-	-	-

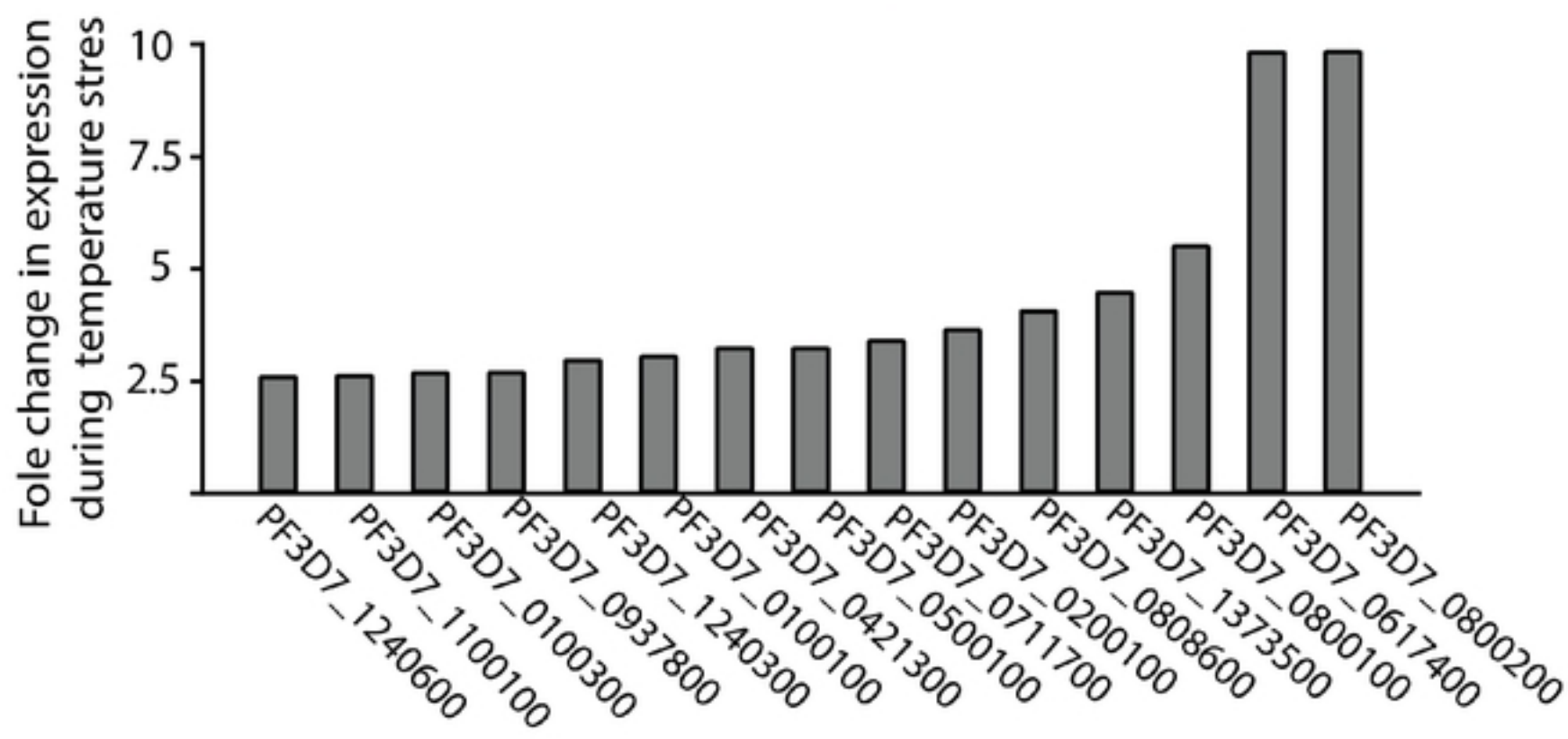
S5A



S5B

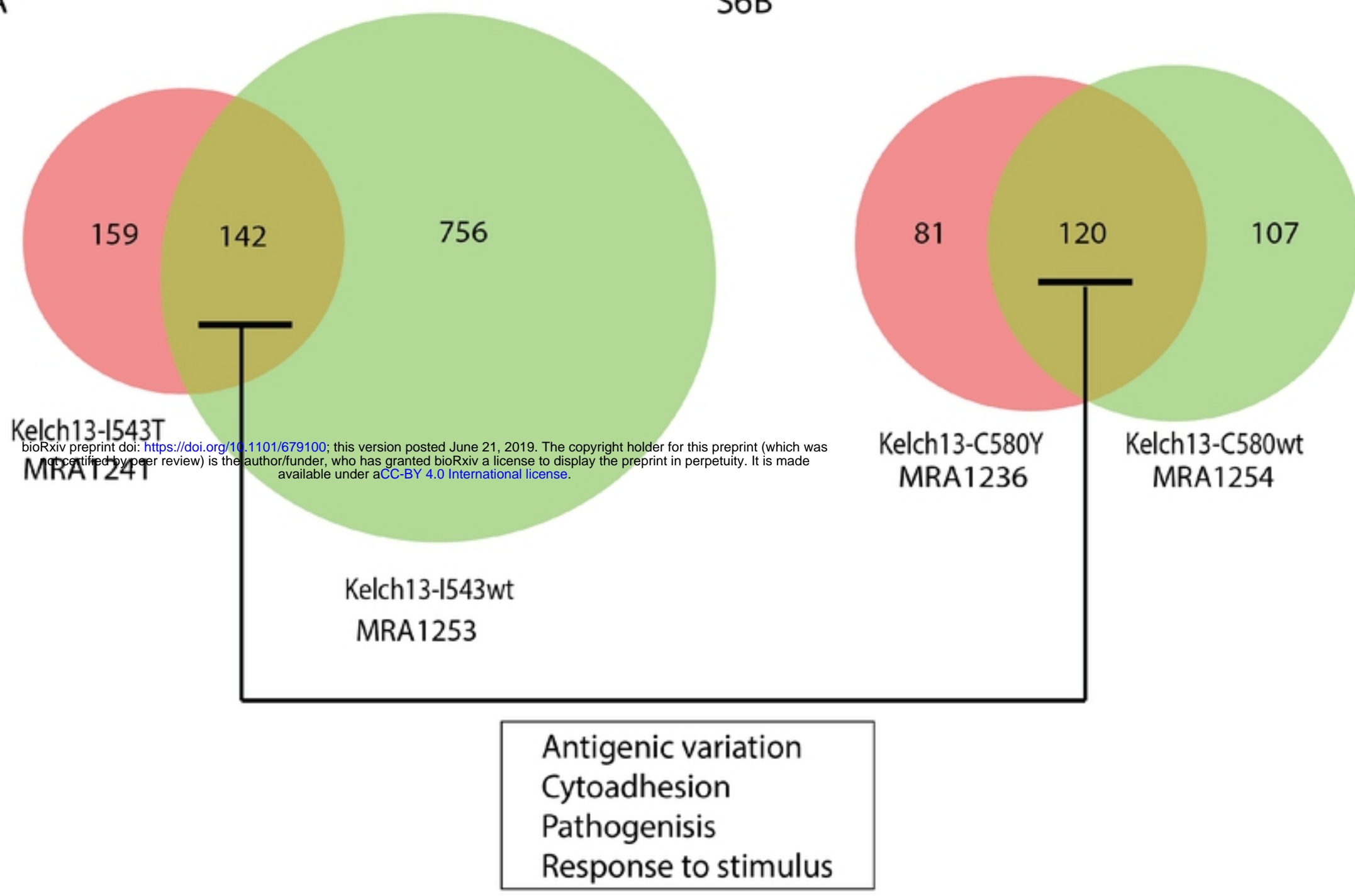


S5C



S6A

S6B



S6C

